

Mercury Control with Calcium-Based Sorbents and Oxidizing Agents

Quarterly Report

Period of Performance:

January 1st, 2003 through March 31st, 2003

Prepared by

Thomas K. Gale

April 2003

DE-PS26-02NT4183

Southern Research Institute
2000 Ninth Avenue South
P. O. Box 55305
Birmingham, AL 35255-5305

Prepared for

Barbara Carney
National Energy Technology Laboratory
United States Department of Energy
626 Cochran's Mill Road
Pittsburgh, PA 15236-0940

Disclaimer

This report was prepared as an account of work sponsored by an agency of the United States Government. Neither the United States Government nor any agency thereof, nor any of their employees, makes any warranty, express or implied, or assumes any legal liability or responsibility for the accuracy, completeness, or usefulness of any information, apparatus, product, or process disclosed, or represents that its use would not infringe privately owned rights. Reference herein to any specific commercial product, process, or service by trade name, trademark, manufacturer, or otherwise does not necessarily constitute or imply its endorsement, recommendation, or favoring by the United States Government or any agency thereof. The views and opinions of authors expressed herein do not necessarily state or reflect those of the United States Government or any agency thereof.

Abstract

The complicated chemistry and multiple mechanisms affecting mercury speciation and capture make it necessary to investigate these processes at conditions relevant to full-scale boilers. Experiments were performed in a 1MW semi-industrial-scale, coal-fired facility, representative of a full-scale boiler. Southern Research Institute's spike and recovery system and procedures were used to obtain real-time gas-phase mercury-speciation measurements, with less than 5% uncertainty in the measured values. The focus of this work was on solutions for Powder River Basin (PRB) sub-bituminous coals and high-burnout conditions, where the fly ash contained relatively little unburned carbon. The relationship of mercury oxidation and capture with chlorine concentration was investigated in conjunction with other associated parameters of importance, such as unburned carbon, minerals in ash, flue-gas composition, and hydrated lime injection. The impact of chlorine content was independently evaluated by injecting chlorine through the burner, while firing PRB coal. The concentration of oxidized mercury at the baghouse inlet and outlet increased as chlorine was added to the flue gas. The sum total of mercury removal also increased with increasing chlorine content. For the high-efficiency (low UBC) conditions investigated in this work, ash composition was found to be more important than chlorine content. The addition of high-iron bituminous ash, either through direct ash injection or through coal blending, was found to significantly increase mercury oxidation and capture before and within the pilot combustor's baghouse, while firing PRB coal. For certain pilot-scale conditions, blending a small amount of high-iron bituminous coal (<20% by mass) with PRB sub-bituminous coal, resulted in oxidized fractions of mercury of >50% before the particulate collection device, >95% at the outlet of a baghouse, and as much as 60% total mercury removal. Not only does the catalytic material in bituminous ash enhance Hg-oxidation, it also directly enhances the capture of oxidized mercury by calcium (i.e., PRB flyash and hydrated lime).

The results from this work suggest several potential Hg-control strategies for coal-fired power plants that produce low UBC, high-calcium flyash (e.g., PRB). First, blending a small amount of bituminous coal with PRB sub-bituminous coal (i.e., 10% by mass) may allow the majority of mercury to be oxidized and then effectively captured by existing control equipment, such as in a scrubber. Second, Hg-capture through optimization of coal-blending may allow near complete capture of mercury without additional mercury control equipment, especially for power-plants that use baghouses. The impact of coal blending on Hg-capture across an ESP remains to be investigated. Finally, direct injection of calcium-based sorbents (i.e., hydrated

lime, dolomite, limestone) into particulate control devices for coals with deficient calcium and direct injection of catalytic material (i.e., bituminous coal ash) for coals with deficient catalytic material may be an effective way to mitigate Hg-emissions.

Section	Table of Contents	Page
Introduction to Mercury Oxidation		5
Experimental Synopsis		6
Results and Discussion of Hg-Oxidation Investigation		12
Summary of Mercury Oxidation Section		21
Introduction to Mercury Capture by Calcium		21
Results and Discussion of Mercury Capture Investigation		22
Summary of Mercury Capture Section		31
Conclusions		32
Future Work		32
<u>Sodium Tetrasulfide</u>		32
<u>ADVACATE Sorbent Multi-Pollutant Control</u>		33
<u>Isolating UBC and Ash Minerals</u>		34
References		35
APPENDIX A EXPANDED EXPERIMENTAL		38
APPENDIX B NON-CORRELATING GRAPHS		43
APPENDIX C RUN CONDITIONS AND DATA		47

Figure	List of Figures	Page
1	Combustion Research Facility (CRF)	6
2	Temperature/time history comparison	7
3	Temperature profile during mercury measurements	8
4	Mercury monitoring system, including spike and recovery	9
5	Mercury speciation data taken with an advanced and customized	10
6	Effect of flue-gas chlorine on Hg-oxidation	13
7	Mercury speciation at the baghouse inlet	14
8	Mercury speciation at the baghouse outlet	14
9	Effect of AeroPulse pulse-jet baghouse temperature on Hg-oxidation	15
10	Influence of UBC on Hg-speciation	16
11	Influence of SO ₂ on Hg-speciation	17
12	Relationship of ash Fe ₂ O ₃ /CaO ratio with Hg-speciation	17
13	Oxidation of mercury across the baghouse while injecting ash	20
14	Total mercury removal while firing PRB coal and Injecting Chlorine	23
15	Total mercury removal as a function of flue-gas chlorine content for blends	23
16	Mercury removal before the baghouse inlet for different blends	24
17	Total mercury removal at baghouse outlet for different blends	25
18	Effect of temperature on the sum total of mercury removal	26
19	Effect of SO ₂ on the sum total of mercury removal	27
20	Effect of UBC and ash minerals on the sum total of mercury removal	27
21	Sum total of mercury removal from injecting Choctaw America coal ash	28
22	Effect of hydrated lime injection for a mostly PRB coal blend	29
23	Fraction of elemental mercury during hydrated lime injection	30
24	Effect of hydrated lime injection while firing Choctaw America coal	31

Introduction to Mercury Oxidation

The predominant forms of mercury in coal-fired flue gas are elemental (Hg^0) and oxidized (HgCl_2) [1-3]. The percentage of oxidized mercury in the stack effluent of a particular power plant depends on many variables associated with the coal type, combustion efficiency, and the pollution control equipment used. Essentially all of the mercury entering the furnace with the coal is vaporized and exists in the elemental form until the flue gases cool below 1000 °F [1-3]. The oxidation of mercury in coal-fired boiler systems is kinetically limited [1-3]. The mercury content of coal is small, and hence, so is the concentration of mercury in flue gas. The trace nature of mercury in flue gas adds complexity to the system of kinetically-controlled reactions that determine the fate of mercury speciation in coal-fired boilers. Because the concentration of mercury is very small in flue gas, any favorable mercury-oxidation reaction does not have the ability to promulgate itself. In virtually every conceivable competitive reaction, the competing gas component, much in excess of mercury, dominates. On the other hand, where the formation of mercuric compounds is thermodynamically favored, bulk and pore diffusion limitations dominate, unless the oxidant is in vast abundance compared with mercury.

In addition to the trace nature of mercury in coal-fired boilers, favorable reactions for mercury oxidation have short temperature/time windows. Consequently, the extent of mercury oxidation is highly dependent on catalytic processes. Heterogeneous catalysis not only enhances the direct mercury oxidation reactions, but also makes available gas components (such as Cl) that are otherwise scavenged by competing gas species present at much higher concentrations. The combination of factors affecting mercury speciation in coal-fired boilers makes it extremely difficult to design a cost-effective strategy for mercury control. The present work attempts to obtain an understanding of the mechanisms governing mercury speciation in flue-gas environments that exist in full-scale utilities. A correct and more complete understanding of Hg-speciation will allow direct design and development of Hg-mitigation technologies and processes with assurance of the desired result.

A system of reactions, which include significant chlorine-speciation reactions, has been proposed to describe homogeneous Hg-oxidation [4]. This set of governing reactions allows direct oxidation of Hg^0 to HgCl and HgCl to HgCl_2 by the following four chlorine species with different reaction rates: Cl, Cl_2 , HCl, and HOCl [4]. This system of equations has been shown to effectively predict mercury speciation for specific homogeneous systems [2]. However, the homogeneous model alone consistently under predicts the oxidation of mercury from coal-fired boilers [5]. Hence, it is important to identify and describe the heterogeneous reactions that dominate the mercury-oxidation process.

Benchscale work has identified several components of flyash that may play an important role in heterogeneous Hg-oxidation reactions [6-7], particularly unburned carbon (UBC) and iron [7]. Niksa et. al. [8] suggested a possible mechanism whereby UBC can catalyze mercury oxidation, as follows:



Chun et. al. [7] performed benchscale Hg-oxidation experiments over different coal flyash and found that coal ash high in iron was particularly effective at catalyzing the mercury oxidation reaction. In analogy to Equ.1 and to other chlorine speciation catalysis enhanced reactions, the iron enhanced mercury oxidation reaction may be represented by:



where FeCS = an iron catalytic site. In both equations 1 and 2 above, HCl is the chlorine species of focus, because this is the predominant form of chlorine in flue gas in all coal-fired boilers. In fact, nearly all chlorine passing through the burner is converted to HCl and remains in that form through the stack exit, as confirmed by experiments [1], thermodynamic equilibrium predictions [1], and kinetic modeling [2]. On the other hand, Cl (attached to the catalytic site) is the most likely candidate for mercury oxidation. Indeed, Cl is considered the form of chlorine that is most responsible for mercury oxidation in coal-fired boilers [9].

In addition to the specific heterogeneous reaction mechanisms suggested in the literature, SO_x and NO_x have been implicated in terms of having an effect on mercury oxidation [3]. Hence, the present work focuses on the effects of UBC and iron in ash and the importance of chlorine and other acid gases on mercury speciation. Experiments were conducted in a 1MW semi-industrial scale coal-fired facility. Therefore, the mechanisms elucidated are believed to be applicable to full-scale units.

Experimental Synopsis

The Combustion Research Facility (CRF) at Southern Research Institute (SRI) in Birmingham, AL, is a 1-MW_t semi-industrial-scale, coal-fired facility, which mimics the thermal profile of a full-scale boiler from the burner through the economizer. Figure 1 shows a two-dimensional sketch of this facility.

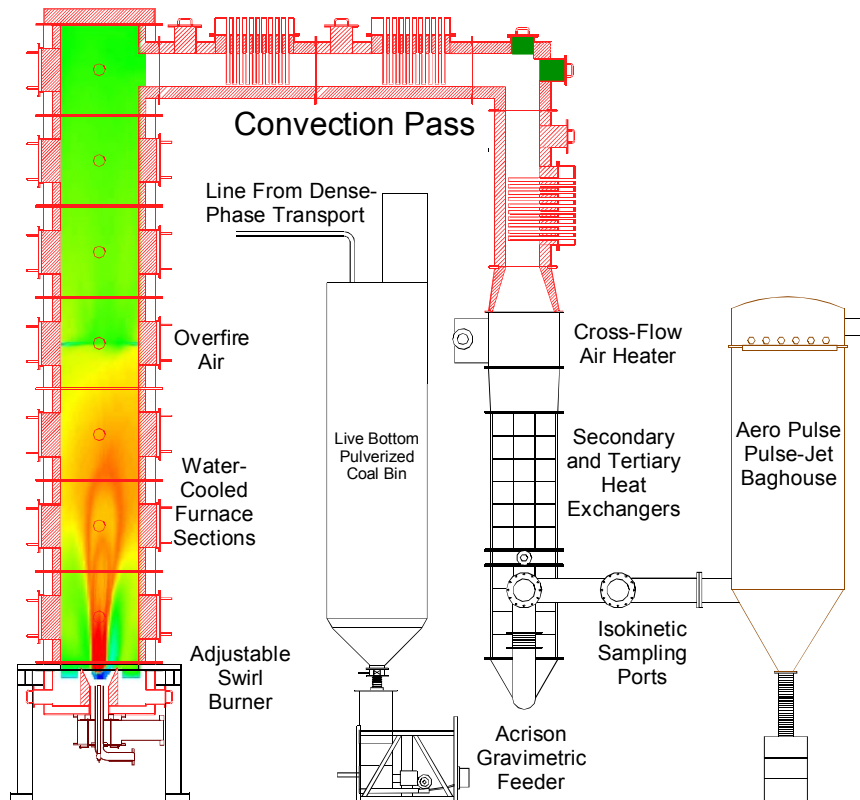


Figure 1. Combustion Research Facility (CRF).

In this work, mercury speciation was measured at the inlet and outlet of an Aero-Pulse pulse-jet baghouse, which uses full-scale Ryton-bags. As shown in Fig. 2, the temperature/time history of the CRF mimics that of full-scale power plants from the burner through the economizer. The data in Fig. 3 illustrate the range of temperature/time histories for all experiments performed in the CRF, in this investigation. Two different baghouse temperature conditions were explored, a high (Inlet = 337 °F, Outlet = 300 °F) and a low (Inlet = 280 °F, Outlet = 260 °F) condition. The baghouse temperature was adjusted by changing the rate of cooling in the last set of heat exchangers, the inlet temperature of which was fairly constant and was always below 550 °F. Several hours were allowed between each change in baghouse temperature to allow the system to reach steady state. The residence time from the burner to the baghouse (identified in Fig. 3) changed by less than a quarter-second across the range of coal-blends and baghouse temperature conditions.

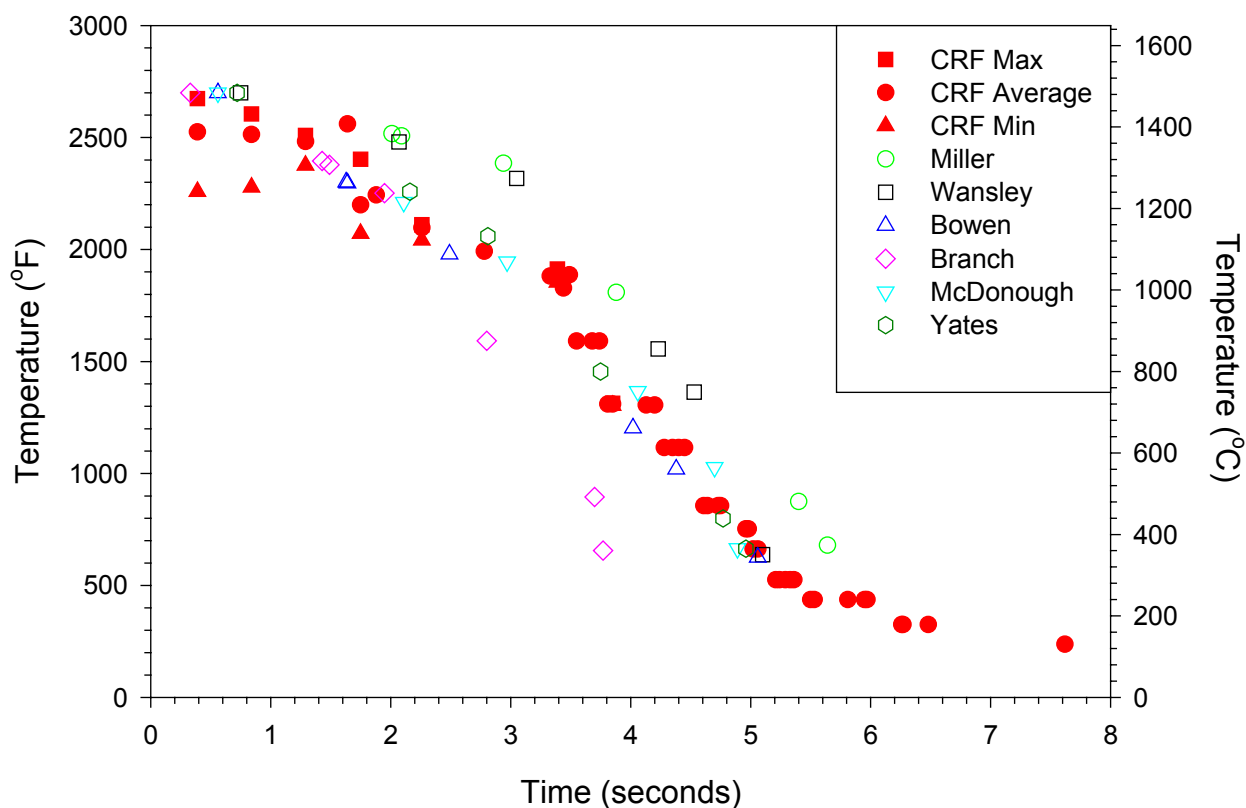


Figure 2. Combustion Research Facility (CRF) temperature/time histories compared with those of full-scale Southern Company coal-fired power plants.

An extractive continuous-emissions monitoring (CEM) system measured the concentrations of CO, CO₂, NO_x, SO₂, and O₂ in the flue gas, just ahead of the baghouse. In addition, manual measurements of chlorine and moisture were obtained throughout the testing.

Mercury monitoring was performed with an advanced and improved version of the PS Analytical 10.665 Stack Gas Analyzer. The PSA monitor has been customized to use an APOGEE Scientific QGIS probe for sampling flue gas. The QGIS probe is designed to pull a large volume of flue gas through an annulus within the probe at a high and turbulent velocity, thus scouring clean the walls of this annulus. The inner wall of the annulus contains a section

with a porous frit through which a small sample of flue gas is drawn. The excess flue gas is directed back into the duct, downstream of the sample inlet. In this way, the QGIS probe allows a sample to be drawn from the duct without pulling it through an ash layer, thereby minimizing alteration of the gas sample – especially capture or oxidation of the vapor phase mercury by or on the particulate. Southern Research also developed an advanced *spike and recovery* system to validate the correctness of the mercury-speciation numbers measured and correct for errors that occur. As a result of these and other modifications, Southern Research Institute believes it can now measure mercury speciation within a maximum uncertainty of 5%. Accurate and precise mercury speciation measurements are key to a fundamental mercury speciation and capture investigation.

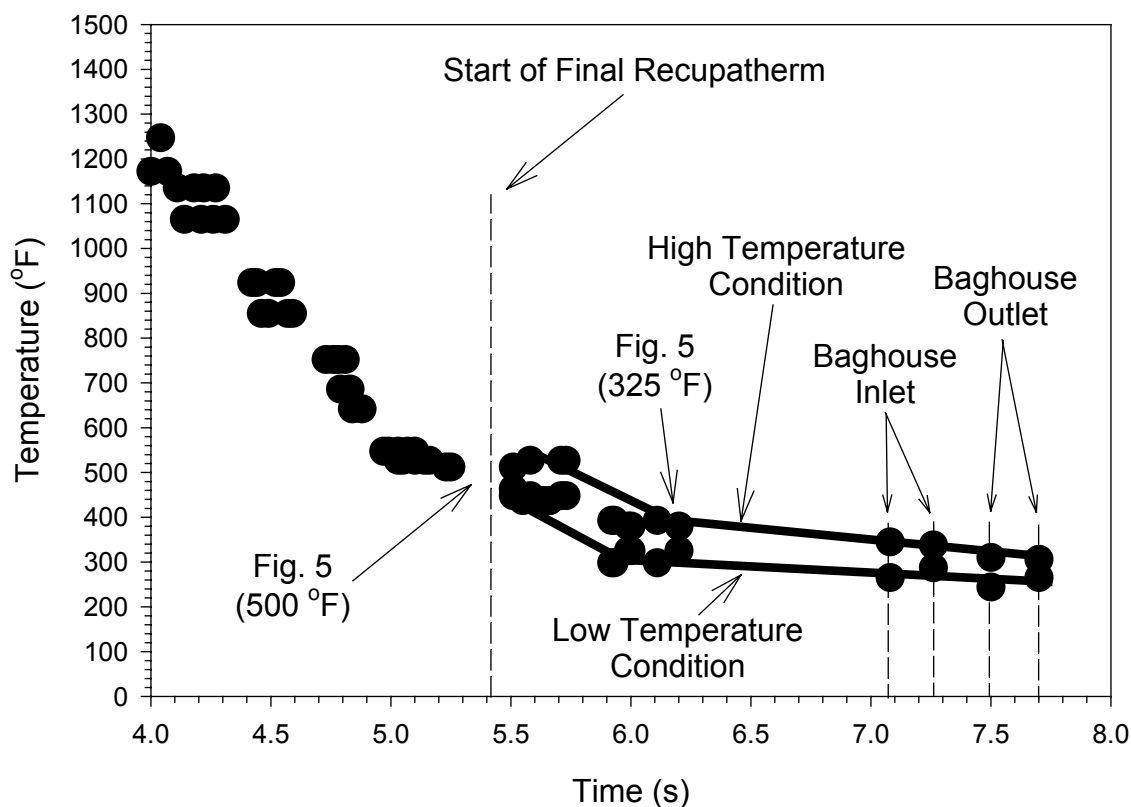


Figure 3. Temperature profile during mercury measurements.

The *spike and recovery* system is a first of its kind prototype provided by PS Analytical. The adaptation of this *spike and recovery* system to allow spiking at the tip of the APOGEE Scientific QGIS probe was performed by Southern Research personnel. The spike of mercury is introduced into the tip of the APOGEE Scientific QGIS probe far enough downstream from the inlet to prevent losses to the duct and far enough upstream of the porous annulus to allow complete mixing before the sampled gas is pulled through the porous frit. A relatively small quantity of air is used to carry the mercury spike to the probe. Therefore, dilution is insignificant, and the general flue-gas composition is undisturbed. The main impact of the spike is simply to increase the concentration of mercury in the sampled gas. This is significant, since mercury-oxidation processes that interfere with speciation measurements can involve three and four component interactions of flue-gas species on catalytic ash sites [10]. The concentration of

mercury in the spike stream is generated by controlling the flow rate, pressures and temperatures of air in and through a mercury reservoir chamber. In addition, SRI uses a parallel Hg-source for the *spike and recovery* system, involving permeation tubes, allowing a check on the source calibration. High-precision mass flow controllers are used to obtain the precise metering needed for high-certainty calibrated spikes. Southern Research believes that *spike and recovery* provides a greater level of confidence in the resulting mercury speciation measurements than any other method currently in use. A schematic of the monitoring system is presented in Fig. 4, including spike location, gas-conditioning system, and calibrated spike source.

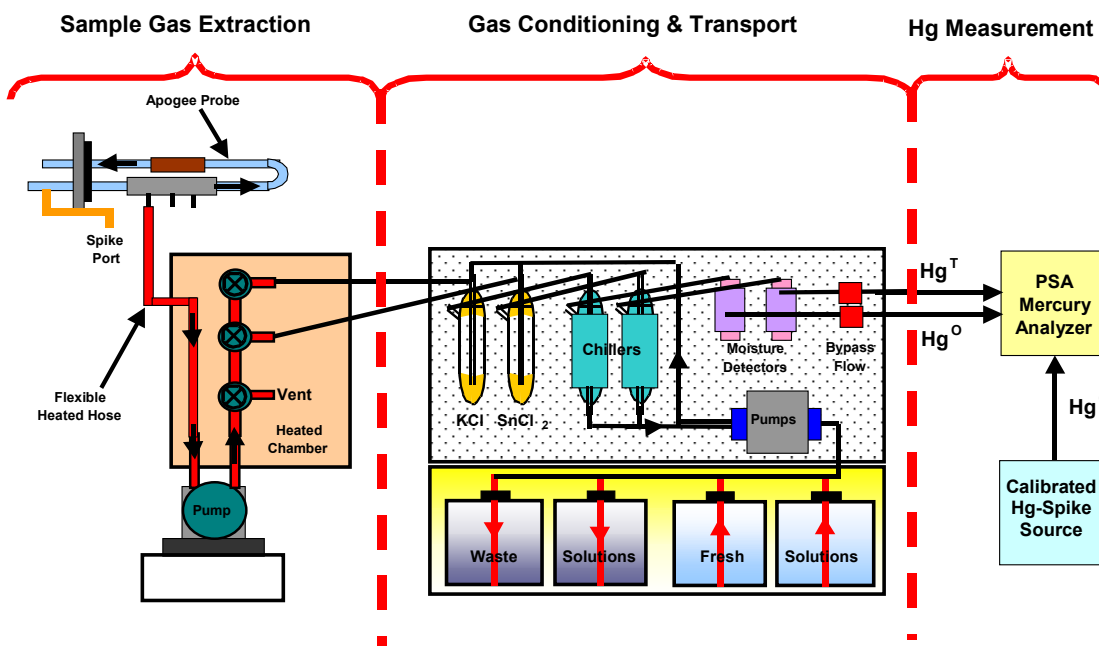


Figure 4. Mercury monitoring system, including spike and recovery.

Figure 5 illustrates the use of the *spike and recovery* system for establishing total and oxidized mercury concentrations in the flue gas, while first burning natural gas (time 0:00 to 5:00) and then Black Thunder, a Powder River Basin (PRB) coal. As shown, the *spike recoveries* are observed on top of the measured initial mercury concentrations for both fuels. The mercury speciation data were obtained well upstream of the baghouse. The residence times at the actual sampling points (temperature locations) are marked on Figure 3. Table 1 contains the Hg-speciation measurements of the PRB flue gas, after correction using the *spike recoveries* shown in Table 2 (explained below).

Table 1. Location and speciation of Hg-measurements, while firing PRB coal.

Location	Temperature (°F)	Hg ^o (μg/Nm ³)	Hg ^T (μg/Nm ³)	Elemental Fraction %
After Recupatherm 1	500	7.4 +/- 0.93	8.4 +/- 1.1	88.1 +/- 1.5
After Recupatherm 2	325	6.5 +/- 0.44	8.0 +/- 0.70	81.3 +/- 1.0

- The mercury concentrations were measured with 6% oxygen in the flue gas.

The percentage of elemental mercury was measured directly (i.e., the population of individual measurements of Hg° and Hg^T , taken one after the other, were used to obtain the average and standard deviation for the elemental fraction), not calculated from the other values in the table.

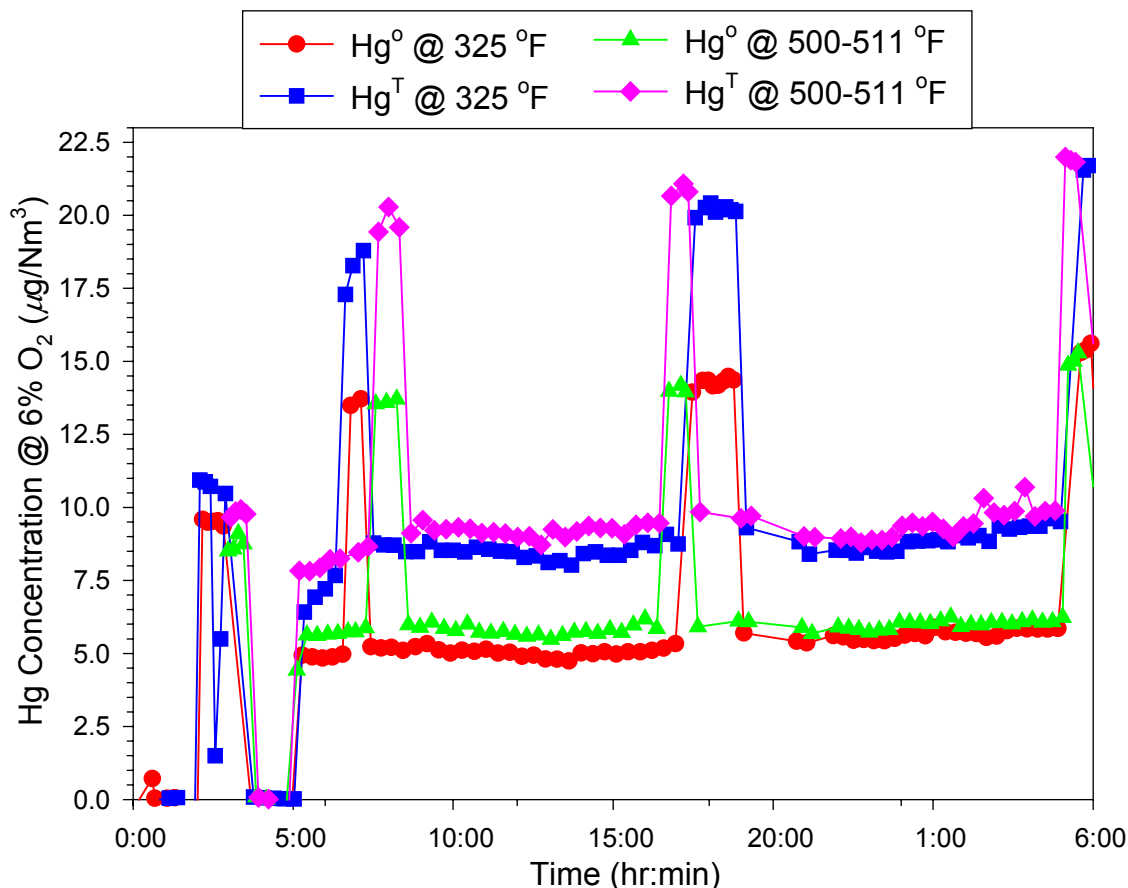


Figure 5. Mercury speciation data taken with an advanced and customized Hg-speciation semi-continuous monitor, and validated with *spike and recovery* for quality assurance.

As shown in Table 2, the recoveries of the elemental-mercury spike are consistently lower than the recoveries of total mercury. This is due to undesired oxidation in the sampling lines and uptake of mercury in the KCl impingers. On the other hand, the stannous chloride (total Hg) impingers scavenge a significant quantity of CO_2 , thus artificially raising the concentration of mercury in the sample gas.

Table 2. Spike recoveries while firing PRB coal.

Sample Type	Temperature (°C)	Recovery 1 ($\mu\text{g}/\text{Nm}^3$)	Recovery 2 ($\mu\text{g}/\text{Nm}^3$)	Recovery 3 ($\mu\text{g}/\text{Nm}^3$)	Ave Recovery /Spike (%)
Hg°	163	8.30	8.78	8.06	86.4
Hg^T	163	10.96	11.13	10.80	113.0
Hg°	260	7.91	8.24	7.81	82.4
Hg^T	260	11.59	11.64	11.06	117.8

- The Hg° spike injected into the tip of the sampling probe was $\sim 9.7 \mu\text{g}/\text{Nm}^3$.

However, with *spike and recovery* these errors can be observed and corrected. In this case (see Table 2), the spike recoveries were all within 20% of the expected value. Hence, a simple linear correction factor was used. As partially apparent in the data of Table 2, the difference in recoveries between expected and actual values was systematic, not random. In addition, as apparent in Fig. 5, there was little variation of the measured data for the flue-gas measurements or the spike-recoveries themselves. Using the *spike and recovery system* to correct for the systematic error has allowed mercury speciation measurements with less than 5% uncertainty for all of the data presented in this paper. This estimate of uncertainty is the standard deviation of corrected values added to the inherent uncertainty of the measurement technique.

Tables 3-5 contain the analysis (including Hg and Cl) of the Black Thunder Powder River Basin Coal (PRB) and two bituminous coals, Choctaw America and Blacksville, used in this work. The PRB coal is the same coal used to obtain the data in Fig. 5. As shown in Tables 3 and 4, both PRB and Choctaw America are low chlorine coals. Blacksville is a higher chlorine coal (see Table 5). Choctaw America was chosen to blend with PRB for two reasons. First, it is a low chlorine coal, so the importance of other parameters could more easily be examined without interference of chlorine. Second, it has a high iron content. As shown in Table 6, Blacksville has an even higher iron content than Choctaw America, which is the primary reason for choosing this coal to blend.

Table 3. Black Thunder PRB Sub-bituminous coal analysis (from coal feeder discharge).

Proximate Analysis (as rec.)		Ultimate analysis (daf)		Hg and Cl Analysis (as rec.)	
% Moisture	14.00	% Carbon	74.55	Hg ($\mu\text{g/g}$)	0.081–0.097
% Ash	5.92	% Hydrogen	4.78		
% Volatiles	37.57	% Nitrogen	1.03	Cl (%)	< 0.010
% Fixed C	42.70	% Sulfur	0.37		
HV (Btu/lb)	9,969	% Oxygen	19.27		

Table 4. Choctaw America HvA Bituminous coal analysis.

Proximate Analysis (as rec.)		Ultimate analysis (daf)		Hg and Cl Analysis (as rec.)	
% Moisture	2.04	% Carbon	85.39	Hg ($\mu\text{g/g}$)	0.08 – 0.10
% Ash	4.19	% Hydrogen	5.16		
% Volatiles	31.76	% Nitrogen	2.04	Cl (%)	0.0127
% Fixed C	62.01	% Sulfur	0.96		
HV (Btu/lb)	14,019	% Oxygen	6.45		

Table 5. Blacksville HvA Bituminous coal analysis.

Proximate Analysis (as rec.)		Ultimate analysis (daf)		Hg and Cl Analysis (as rec.)	
% Moisture	4.03	% Carbon	84.00	Hg ($\mu\text{g/g}$)	0.09
% Ash	8.49	% Hydrogen	5.40		
% Volatiles	37.01	% Nitrogen	1.67	Cl (%)	0.0580
% Fixed C	50.47	% Sulfur	3.10		
HV (Btu/lb)	13,299	% Oxygen	5.84		

Table 6. Mineral analysis of parent coals

Species	Black Thunder	Choctaw America	Blacksville
% Li ₂ O	0.01	0.06	0.03
% Na ₂ O	1.4	1.1	1.0
% K ₂ O	0.50	2.0	2.9
% MgO	4.3	1.1	1.0
% CaO	22.0	2.5	4.6
% Fe ₂ O ₃	6.0	13.8	21.1
% Al ₂ O ₃	15.4	31.4	21.3
% SiO ₂	35.4	42.6	41.6
% TiO ₂	1.3	1.3	1.2
% P ₂ O ₅	0.70	0.16	0.08
% SO ₃	11.5	2.8	4.8

See Appendix A for further details on the experimental.

Results and Discussion of Hg-Oxidation Investigation

Many different parameters are altered when coal-blend and firing conditions are changed. However, the coal mercury content was fairly consistent (see Tables 3-5), and operation of the CRF was stable. Therefore, the main differences in conditions fall within two broad categories, flue-gas composition and flyash properties. The likely parameters of importance are UBC, iron and calcium content, availability of catalytic material, total flue-gas chlorine content, moisture, SO₂, NO_x, and surface area. The other large-volume benign parameters (i.e., O₂, CO/CO₂, etc.) were visually examined for a correlation with Hg-oxidation in plots similar to those shown in the remainder of this report, but none were found. Of the likely parameters, NO_x and moisture were found not to have any observable correlation to mercury oxidation in this work (see Appendix B). The remaining likely parameters were examined, and their relationship to mercury oxidation is illustrated and discussed in this section.

Figure 6 compares the relationship between gas-phase Hg-speciation and chlorine when the flue gas HCl is varied either by injecting chlorine through the burner while firing PRB coal or by blending PRB with higher chlorine bituminous coals. All data presented in this and all remaining figures are corrected to 8% oxygen in the flue gas, which was the average oxygen level in the flue gas at the baghouse inlet. Thus all of the values presented are directly comparable, one to another. In Fig.6, the vertical axis is the fraction of gas-phase elemental mercury found at either the baghouse inlet or outlet divided by the total gas-phase mercury found at the baghouse inlet. The mass balance on coal-mercury suggests that the majority (>80%) of mercury injected with the coal was in the gas-phase at the baghouse inlet for all blend conditions. It was assumed that any elemental mercury captured in the baghouse would have been first oxidized. It was also assumed that reduction of mercury from the oxidized to elemental form across the baghouse was insignificant. The conventions described for Hg⁰/Hg^T at the inlet and outlet of the baghouse, shown in Fig. 6, were also used for all remaining graphs in this report.

As shown (see Fig. 6), chlorine injection through the burner of the CRF decreased the fraction of elemental mercury at the inlet and outlet of the baghouse. However, the elemental mercury fraction at the inlet and outlet of the baghouse during coal blending (with the same concentration of HCl in the flue gas) is much less than that observed while firing PRB coal only.

This step change in Hg-oxidation between 100% PRB and PRB/bituminous blends, suggests a change of controlling Hg-oxidation mechanisms. The values in Fig. 6 are not significantly affected by differences in furnace exit oxygen (FEO) levels, which has an effect on UBC.

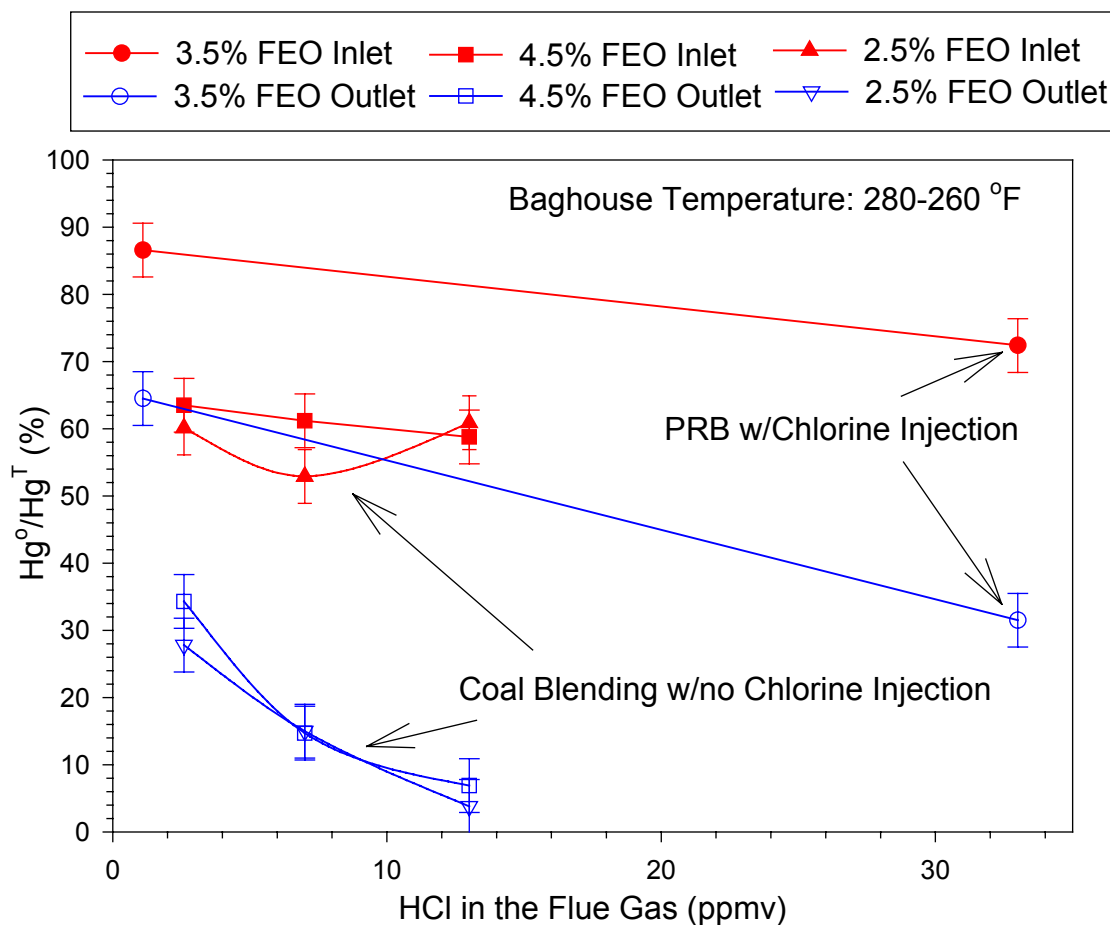


Figure 6. Effect of flue-gas chlorine on Hg-oxidation at the baghouse inlet and outlet for several different levels of furnace exit oxygen (FEO).

Figure 7 illustrates the extent of mercury oxidation at the inlet of the baghouse for 3 different coal blends at two different FEO levels. For comparison, a line is drawn in Fig. 7 at ~ 86.6%, representing the fraction of mercury in the elemental form for 100% PRB at 3.5% FEO and approximately 1 ppm HCl. The differences in elemental mercury fraction between different coal blends is small compared with the step decrease in elemental mercury between the 100% PRB case and the coal blend cases, which is about 30%. In general, lower FEO corresponds with higher UBC, but there is very little difference in the fraction of elemental mercury between the 4.5% FEO (UBC: 0.72-0.34) and 2.5% FEO (UBC: 1.45-0.33) data. Flue gas chlorine is also indicated on Fig. 7 (from coal chlorine). It is apparent that oxidation was not dominated by chlorine content in the flue gas. In addition to the variables listed in Fig. 7, the ash composition (i.e., iron and calcium content) differed for each blend.

At the baghouse outlet (see Fig. 8), the extent of mercury oxidation was much greater, indicating significant catalytic enhancement through the baghouse filter cake. Again, the

elemental mercury fraction for 100% PRB coal is much higher than all of the coal blend results. This step decrease in elemental mercury at the front and back of the baghouse suggests that there was a change in mechanisms controlling mercury oxidation between 100% PRB firing and all coal-blend conditions.

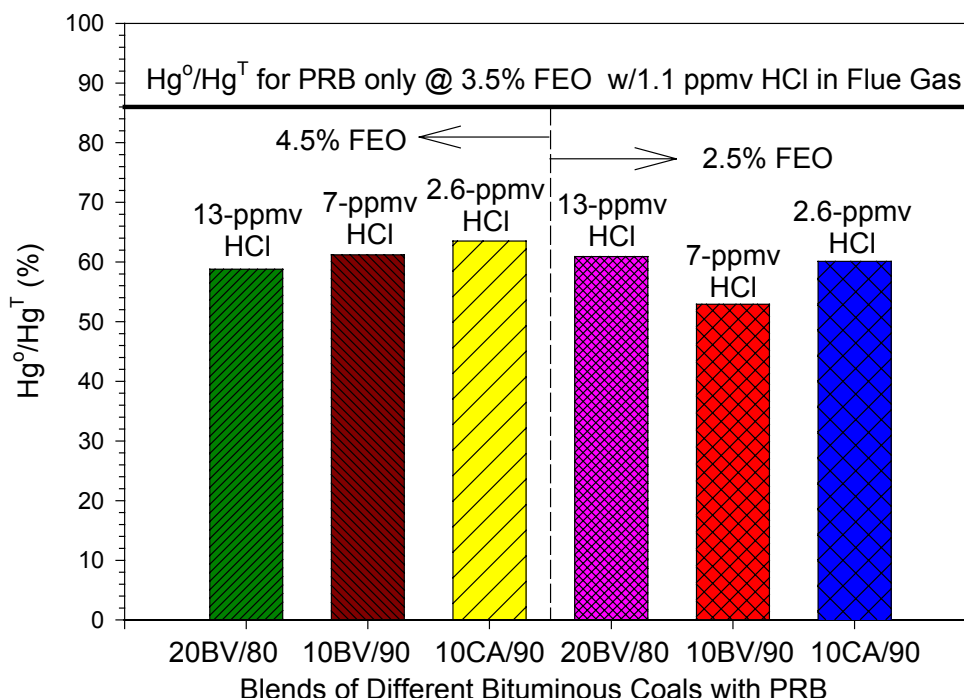


Figure 7. Mercury speciation at the baghouse inlet (@280 °F) for different blends of PRB and bituminous coals (BV = Blacksville, CA = Choctaw America).

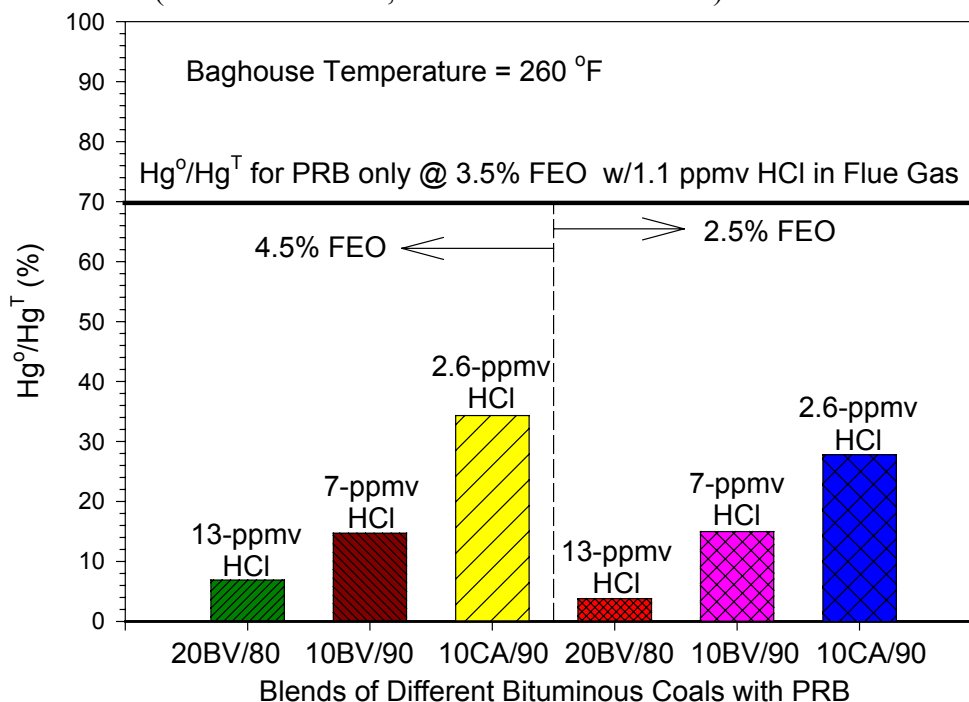


Figure 8. Mercury speciation at the baghouse outlet (@260 °F) for different blends of PRB and bituminous coals.

Significant Hg-oxidation and/or removal occurred across the baghouse while firing PRB coal only (see Figs. 6-8). Apparently, the PRB ash in the baghouse filter cake promotes some catalytic oxidation and/or sorption of elemental mercury. The extent of Hg-oxidation across the baghouse also correlates somewhat with flue-gas chlorine content (see Figs. 6 and 8) when the chlorine is varied by firing different blends. However, chlorine content and the extent of bituminous ash (high iron ash) in the blends are related. It is significant that the elemental mercury reduction across the baghouse increased from an Hg^0/Hg^T level of ~30% to >95% at the baghouse exit, when blending only 20% of Blacksville coal by mass with PRB coal. Unlike the baghouse inlet, the concentration of elemental mercury at the baghouse outlet was less for all coal blends while operating at 2.5% FEO. Therefore, it appears that increased UBC in the ash, during operation at 2.5% FEO, promoted oxidation and/or removal of elemental mercury across the filter cake.

Figure 9 illustrates the relationship of baghouse temperature with elemental mercury fraction at the inlet and outlet of the baghouse, for the particular baghouse conditions of this investigation. The baghouse temperature was changed by adjusting the cooling rate in the final set of heat exchangers. Hence, the change in baghouse temperature affected the flue-gas temperatures upstream of the baghouse (see Fig.3), at the baghouse inlet, and at the baghouse outlet. In addition, using this method to adjust baghouse temperature avoided the convoluting effect of changing moisture content.

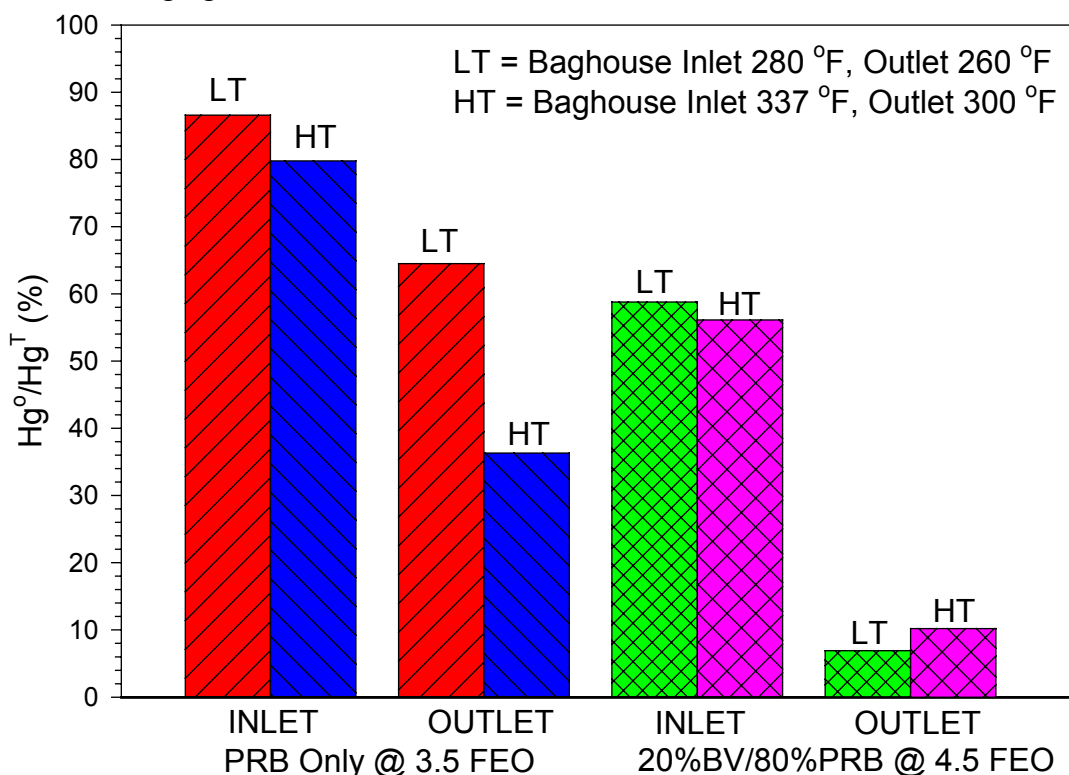


Figure 9. Effect of AeroPulse pulse-jet baghouse temperature on Hg-oxidation.

The small differences in Hg^0/Hg^T -ratio (at the baghouse outlet) were obtained one after the other, by raising and subsequently lowering the baghouse temperature. For example, the low temperature condition was measured, followed by immediate change in heat extraction from the

flue gas and rapid increase in baghouse temperature. An immediate change in the $\text{Hg}^{\circ}/\text{Hg}^{\text{T}}$ -ratio was observed and measured for several hours. Finally, heat extraction was altered to return to the low-temperature condition, and the mercury ratio values returned to the low-temperature values previously measured. In this manner, errors associated with small operational differences from one run to another were eliminated. The standard deviations of the $\text{Hg}^{\circ}/\text{Hg}^{\text{T}}$ ratios directly measured in this work were less than $\pm 1\%$. Hence, while the differences observed as a function of temperature for the coal blend were not large, they were statistically relevant.

The higher temperature is slightly more effective at oxidizing mercury at the baghouse inlet, for 100% PRB coal (see Fig. 9). This effect (for 100% PRB) seems to be enhanced by the baghouse, as the elemental mercury fraction at the baghouse outlet for the higher temperature sample is approximately half the low-temperature value.

The difference between low- and high-temperature oxidation was smaller for the coal blend; i.e., the high-temperature condition did not increase mercury oxidation in the coal blend as it did with 100% PRB. This shift in temperature-dependent behavior is further indication that the mechanisms governing mercury oxidation are different between the 100% PRB case and the coal blends. While the differences in $\text{Hg}^{\circ}/\text{Hg}^{\text{T}}$ -ratio (at the baghouse outlet) were repeatable, they were very small. Therefore, the mercury oxidation effects of flue gas and/or flyash may not be as dependent on temperature with blends as they seem to be with 100% PRB for the specific conditions of this investigation.

Figures 10-12 illustrate a lack of correlation of Hg-oxidation at the baghouse inlet with UBC, SO_2 , or iron/calcium ratio, at the low-temperature condition. This correlation absence was also observed for all ash and flue-gas components.

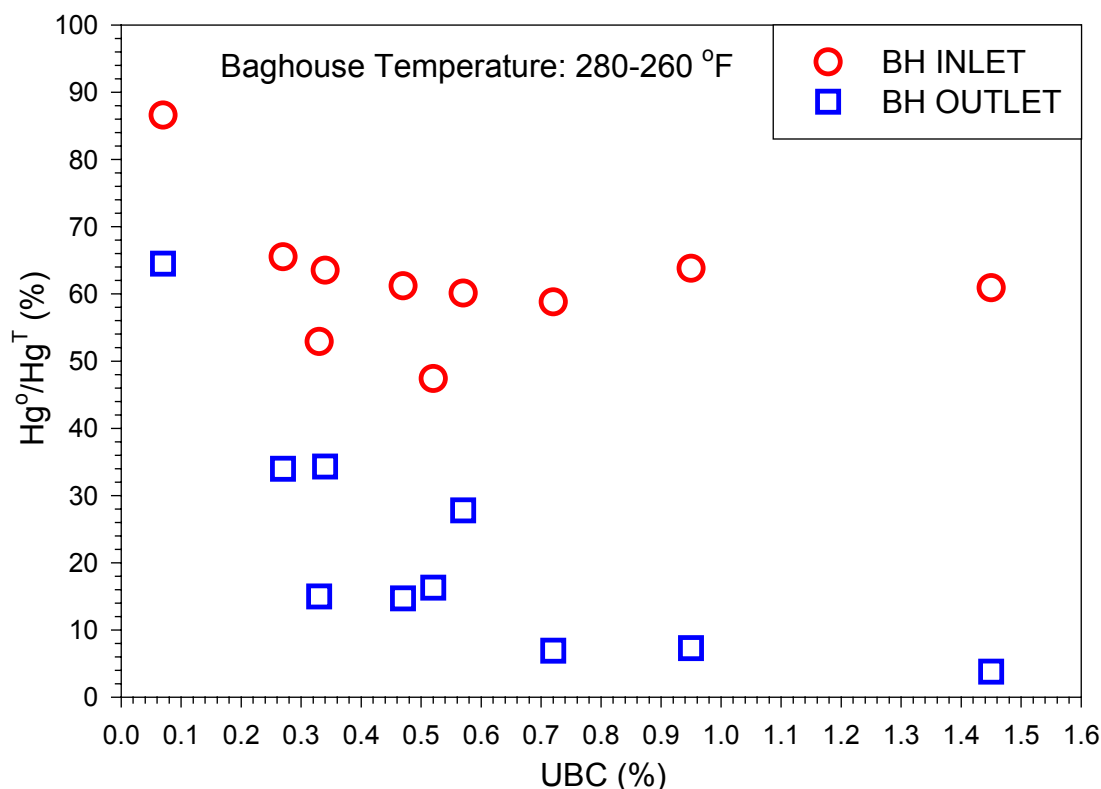


Figure 10. Influence of UBC on Hg-speciation.

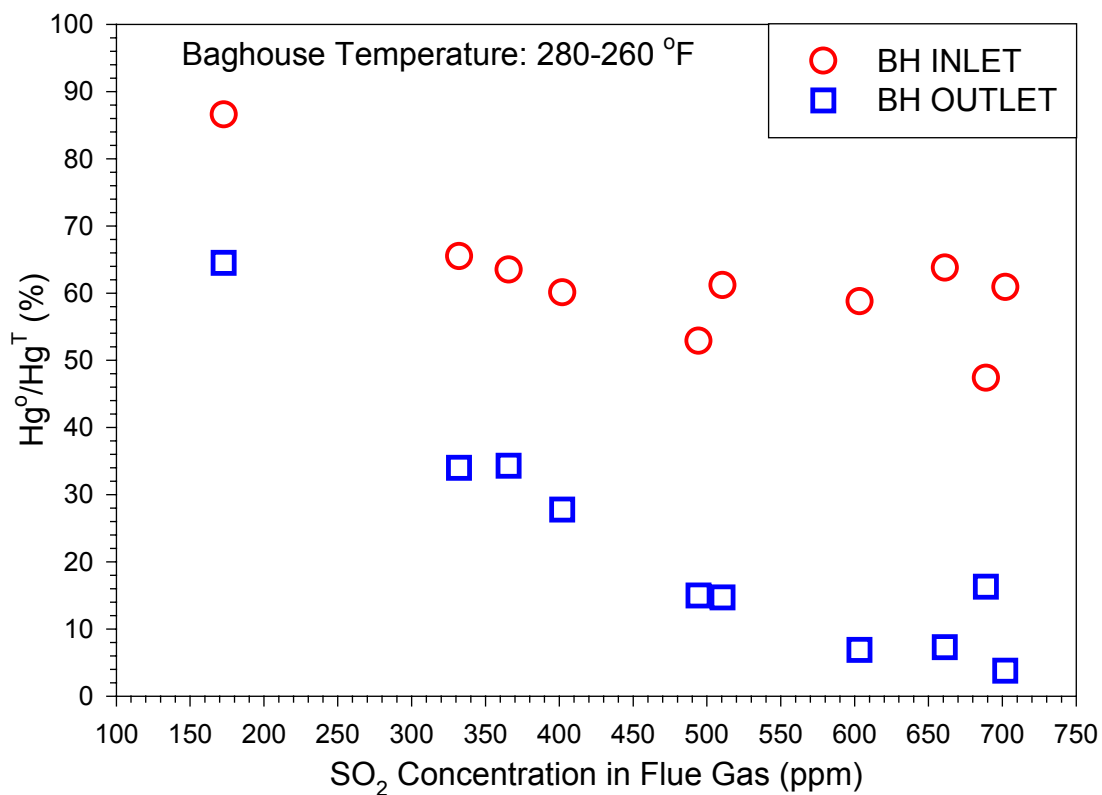


Figure 11. Influence of SO₂ on Hg-speciation.

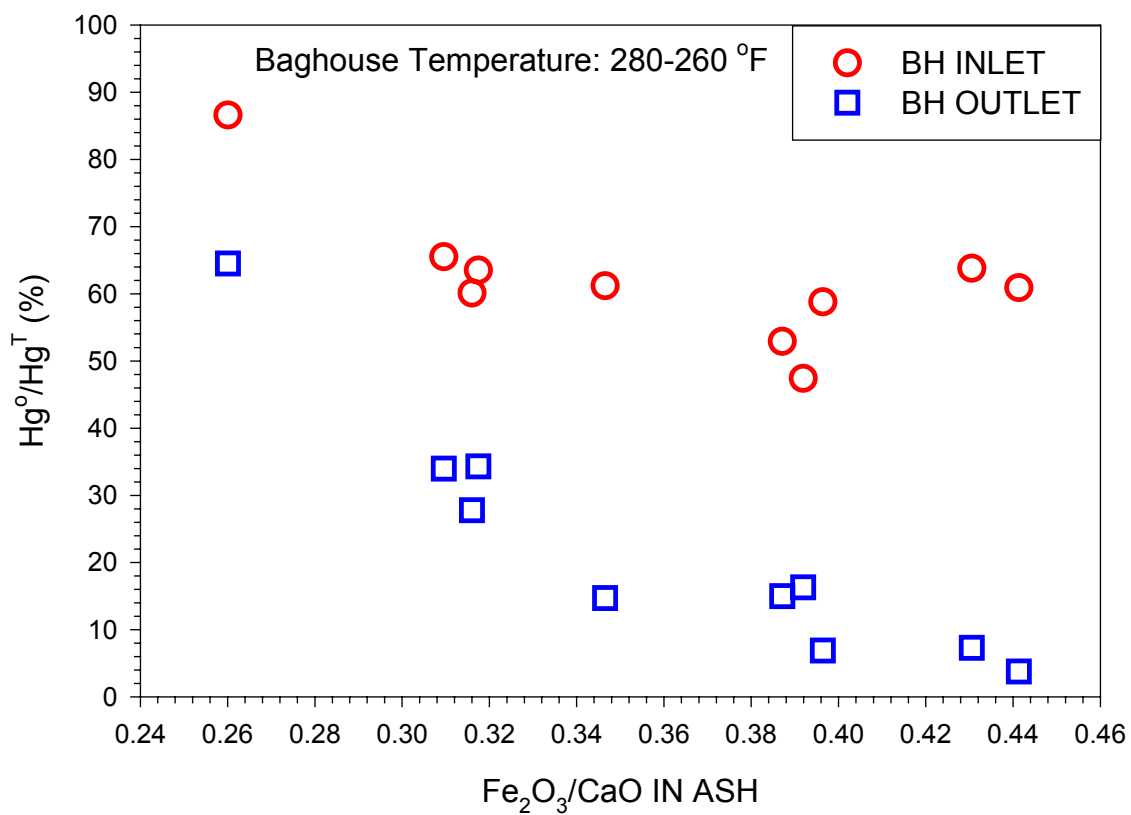


Figure 12. Relationship of ash Fe₂O₃/CaO ratio with Hg-speciation.

Figure 10 indicates a moderate correlation between Hg-oxidation and UBC, at the baghouse outlet, but this correlation is confounded by the association of UBC with other coal-blending parameters. As the amount of bituminous coal is increased in the blend, so does UBC, SO₂, iron, and chlorine. However, as shown in Fig. 8, lower FEO levels, which produce higher UBC, yielded slightly less elemental mercury at the baghouse outlet. PRB generally produces low-UBC flyash, and the efficient operation of the CRF produced low UBC flyash values (< 1.5%) for all coal blends. However, for less efficient boilers and/or for those burning bituminous coals, UBC may play a more dominant role.

Figure 11 indicates a significant correlation of mercury oxidation (including any baghouse removal of Hg^o) with SO₂ at the baghouse outlet. However, SO₂ also correlates with the increase in the fraction of bituminous coal in the blend, which in turn corresponds with the alteration of the flyash. Table 7 shows the isokinetically-sampled ash mineral analysis, UBC, and LOI, for the PRB and four PRB/bituminous blends examined in this work. The elemental compositions are very similar. The PRB coal tested had a significant amount of iron in the ash. Although the two bituminous coals contained significantly more iron than PRB (see Table 6), the increase in total iron content of the blends was small. However, the form and availability of iron in PRB ash may be much different than in the bituminous coals. In addition, activity and availability of catalytic materials (such as iron) is more important than the elemental composition of the ash. Therefore, the relationship between mercury oxidation and the iron/calcium ratio was examined (see Fig. 12). This ratio is the best indication of the relative amount of bituminous coal iron in the ash, since both bituminous coals were higher in iron and lower in calcium than the PRB coal. As shown in Fig. 12, a smooth and significant correlation exists between the elemental mercury fraction at the baghouse outlet (again, measured relative to the Hg^T level at the inlet) and the addition of bituminous-coal iron to the flyash. Less than 5% of the mercury entering the baghouse exits in the elemental form for the highest iron/calcium ratios (see Fig. 12).

Table 7. Analysis of isokinetically sampled ash, for blends of PRB with bituminous coals.

Component	100% PRB	Blend 1	Blend 2	Blend 3	Blend 4
% Li ₂ O	0.01	0.02	0.02	0.02	0.02
% Na ₂ O	2.4	1.7	1.9	2.1	1.7
% K ₂ O	0.61	0.70	0.58	0.59	0.74
% MgO	5.3	3.8	4.2	4.4	4.0
% CaO	27.3	21.6	22.8	25.2	22.2
% Fe ₂ O ₃	7.1	9.3	7.9	7.8	8.7
% Al ₂ O ₃	18.2	20.6	21.2	20.7	21.3
% SiO ₂	29.6	34.5	31.2	29.9	34.1
% TiO ₂	1.7	1.6	1.6	1.8	1.6
% P ₂ O ₅	1.30	1.1	1.5	1.5	0.95
% SO ₃	3.7	4.3	5.1	4.8	3.4
% LOI	0.23	0.94	0.36	0.59	0.92
% UBC	0.04-0.07	0.72-1.45	0.33-0.47	0.27-0.57	0.51-0.53

The step change in Hg-oxidation between 100% PRB (see the two leftmost data points in each plot) and the coal blends has been observed in Figs. 6-12. The correlations in Figs. 10-12 suggest mechanisms responsible for this step change, because the 100% PRB data points seem to

fall into line with the correlation for the coal blends (particularly for the baghouse outlet). This suggests that UBC, SO₂, the added bituminous coal iron, or a combination of these parameters is responsible for the change in mechanisms observed between the 100%-PRB condition and all coal-blend conditions.

Heterogeneous Hg-oxidation mechanisms are associated with particulate material, which plays a more dominant physical role in the ash-cake coating bag surfaces than in the disperse phase. On the other hand, sulfur dioxide may play as dominant of a role in homogeneous mechanisms as in heterogeneous mechanisms. Nevertheless, the relationship of Hg-oxidation to bituminous ash in a dust cake and SO₂ in the flue gas are confounded by the fact that SO₂ and bituminous ash content are related for the coal blends investigated in this work. Hence, it was necessary to experimentally isolate these two parameters. This was done in part by directly injecting high-iron flyash into the baghouse, without adjusting the SO₂ concentration or any other parameters. Ash from the same Choctaw America coal used in this work was selected for this experiment. Its composition is provided in Table 8, along with a comparison of its internal surface area with that of PRB ash. As shown (see Table 8), the surface area is small and similar to PRB ash, while the iron content is high. However, as discussed above, the PRB coal investigated has a moderately high iron content as well (see Table 6). The impact of injected ash may be a function of the *form and availability of the iron* as well. The UBC level, while relatively small for bituminous coal ash from typical full-scale power plants, is significantly higher than for the PRB ash (see Table 7).

Table 8. Analysis of Choctaw America coal ash injected into baghouse.

Mineral Analysis		Other Properties	
% Li ₂ O	0.06	LOI	4.2 %
% Na ₂ O	1.4		
% K ₂ O	2.0		
% MgO	1.2	UBC	3.51 %
% CaO	3.9		
% Fe ₂ O ₃	12.4	meso-pore N ₂ -BET Surface Area	2.32 m ² /g
% Al ₂ O ₃	33.0		
% SiO ₂	43.1		
% TiO ₂	1.8	---	<u>PRB Ash Surface Area</u> 2.02 m ² /g
% P ₂ O ₅	0.38		
% SO ₃	0.53		

LOI = Loss On Ignition, UBC = Unburned Carbon

Figure 13 contains the results of the baghouse ash injection tests conducted at the high-temperature (337 °F to 300 °F) baghouse condition, which is most favorable for elemental-mercury removal (oxidation and/or sorption) by PRB flyash (see Fig.9). The baseline case of PRB-only was compared with three different baghouse injection conditions, 100% Choctaw ash, and two blends of Choctaw ash with hydrated lime, 20% Choctaw ash/80% hydrated lime and 50% Choctaw ash/50% hydrated lime. Particulate was injected into the baghouse at a rate approximately equal to the mass rate of flyash flowing into the baghouse from the furnace. The baghouse was pulsed down at the beginning of each new injection condition, to avoid excessive buildup of material or long transition times from a previous condition. Approximately the same mass rate of particulate was used for each baghouse injection condition.

Hydrated lime has a surface area ($\sim 18 \text{ m}^2/\text{g}$) much greater than that of Choctaw ash (see Table 8). Therefore, the influence of ash composition could be distinguished from the mere increase in mass loading or surface area. As shown in Fig. 13, the injection of 100% Choctaw ash significantly enhanced the oxidation of mercury across the baghouse. Hydrated lime was relatively benign in its effect on Hg-oxidation. As illustrated in Fig. 13, Hg-oxidation increased with increasing concentration of Choctaw ash. The hydrated lime acted merely to dilute the impact of injecting Choctaw ash. It is clear that the catalytic properties of the high-iron ash were important in the oxidation of mercury across the baghouse. It is likely that the bituminous ash iron and UBC were important catalytic components that promoted mercury oxidation in the baghouse. However, the extent of the influence of SO_2 on Hg-oxidation for the coal-blends investigated is uncertain. This will need to be examined further in subsequent experiments.

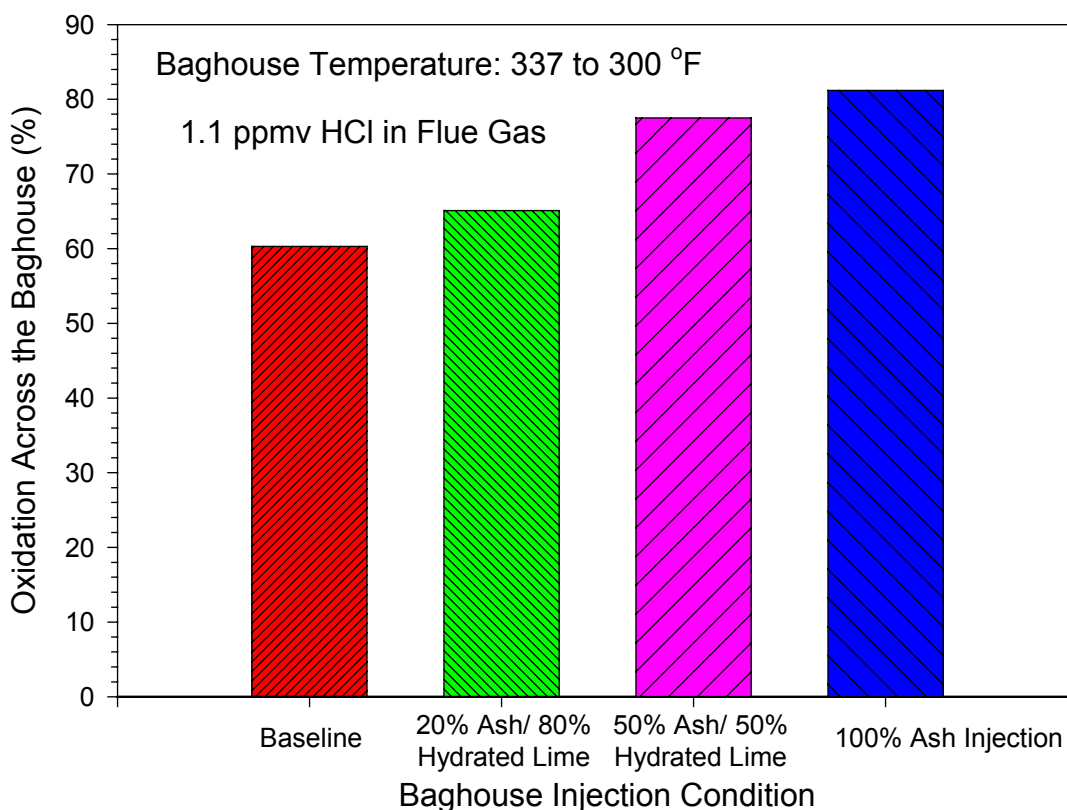


Figure 13. Oxidation of mercury across the baghouse while injecting ash and hydrated lime directly into the baghouse.

The high-temperature baghouse condition, used for the direct ash-injection tests was more favorable for baseline (PRB only) Hg-oxidation (see Fig. 9). However, the low-temperature condition was more favorable for enhancement of Hg-oxidation by the coal blends (see Fig. 9). Therefore, the impact of direct ash injection on Hg-oxidation at the lower temperature condition would likely be more dramatic.

Summary of Mercury Oxidation Section

Total chlorine content, injected independently through the burner or inherent in the coal, tends to increase mercury oxidation in the disperse phase, prior to the baghouse, and across (examined by total Hg^0 reduction) the baghouse (ash cake and filter media). However, in terms of differences observed between PRB sub-bituminous coals and bituminous coals in full-scale boilers, catalytic enhancement by the fly ash is a more important factor in determining the extent of mercury oxidation than the flue gas total chlorine content. PRB-ash (and possibly the bag fabric) captures and/or catalytically enhances the oxidation of mercury across the baghouse, which enhancement increases significantly (~30%) with small increases in temperature (~ $\Delta 40^\circ\text{F}$). The catalytic activity of low-UBC bituminous ash is greater than that for low-UBC PRB ash. UBC, even at the low levels investigated in this work, appeared to have some catalytic effects on mercury speciation, with the activity of relatively low-UBC bituminous ash being greater than the very-low-UBC PRB ash. For less efficient combustion conditions, UBC may play a more dominant role in Hg-oxidation. The iron content and form in bituminous ash may be an important component of its catalytic activity; elemental mercury reduction across the baghouse was observed to increase with addition of bituminous-ash iron, although the change to total iron in the ash was small. Hence, the catalytic activity and availability of iron appears to be important and may differ between coal types. The role of SO_2 on Hg-oxidation will be investigated further in the future.

These results suggest that coal blending may play an important role in mercury mitigation strategies of the future, but substantially more data are needed to confirm this hypothesis and understand the governing processes well enough to rely on such an approach as a compliance strategy. In this pilot combustor, and with these fuels, blending a small amount of bituminous coal (<20% by mass) with PRB sub-bituminous coal, resulted in oxidized fractions of mercury of >50% before the particulate collection device and >95% at the outlet of a baghouse. These results were achieved while maintaining UBC at reasonable levels.

Introduction to Hg-Capture by Calcium

Calcium-based sorbents have shown the ability to capture mercury in fundamental benchscale investigations [11], pilot-scale evaluations [12], and full-scale units [13]. However, Powder River Basin (PRB) coals, high in calcium, are ineffective at either oxidizing or capturing mercury from the flue gases it produces [14]. This is partly due to the fact that PRB coal does not contain the necessary catalytic material, such as UBC or catalytic minerals, necessary to enhance the mercury oxidation rate, as discussed in the previous section. Attempts have been made to promote the oxidation of mercury in PRB flue gas [15] in hopes that once the mercury is oxidized, the high-calcium PRB Ash may capture it. In addition, calcium-based sorbents have been derived with oxidant additives in an attempt to simultaneously oxidize and capture mercury [16]. Even activated carbon sorbents have been fit with oxidant additives in an attempt to enhance their capability to capture mercury [17]. To date, attempts to scale-up the use of sorbents with oxidants to pilot- or full-scale have not been successful [1, 12, 13], particularly on PRB coal. This lack of success has led to the promotion of activated carbon as a mercury mitigation technology. Activated carbon is very expensive [1, 18], derived from limited feedstocks, and contaminates all the flyash, even for very small injection rates [18]. PRB ash contaminated with activated carbon must be deposited in a landfill at high cost, instead of being

sold as a high-value byproduct, which it would otherwise be. Activated carbon injection tests themselves have met with limited success [18].

Many power plants burning bituminous coal, produce ash with high UBC levels, which is often effective at either promoting mercury oxidation or (at very high UBC levels) capturing the mercury directly. PRB coal however, generally produces ash with a much smaller carbon content, which is a major selling point for the ash to the cement industry. While PRB coal ash does not contain high amounts of bituminous-like minerals, it does contain high quantities of calcium, which can itself be an effective sorbent [11], as mentioned above. This section describes the results of an investigation designed to elucidate the mechanism associated with mercury capture by calcium, particularly PRB flyash (a high-calcium sorbent). A greater understanding of the mechanisms controlling capture of mercury by PRB and other forms of calcium in coal-fired flue gas will lead directly to effective and economical mercury mitigation processes and technologies.

Results and Discussion of Mercury Capture Investigation

In the preceding section, the fraction of elemental mercury (Hg^0/Hg^T) at both the inlet and outlet of the baghouse was defined relative to the total mercury (Hg^T) at the baghouse inlet. This was reasonable, since the removal or loss of mercury prior to the baghouse inlet was less than 20% for all conditions examined in the section on mercury oxidation. In addition, the focus of that section was on oxidation rather than removal. For the discussion on mercury removal however, total removal before and after the baghouse is defined relative to the total mercury (Hg^T) fed with the coal. A mass balance on coal mercury compared well with measured baseline (i.e., PRB only and similar conditions) baghouse inlet measurements. Mercury removal values for this section are defined as follows:

$$\text{Before Baghouse Removal} = (Hg^T - Hg_{in}^T)/Hg^T$$

$$\text{Across Baghouse Removal} = (Hg_{out}^T - Hg_{in}^T)/Hg_{in}^T$$

$$\text{Sum Total of Mercury Removal} = (Hg^T - Hg_{out}^T)/Hg^T$$

Hg^T = total mercury based on mercury fed with the coal (and confirmed by measurements)

Hg_{in}^T = the total gas-phase mercury measured at the baghouse inlet

Hg_{out}^T = the total gas-phase mercury measured at the baghouse outlet

Total mercury, as it is used in this section, refers to all forms of mercury in the gas phase, regardless of speciation. Total mercury removal, refers to the removal of all forms of mercury from the gas-phase, regardless of the products formed. The error bars in Figs. 14 and 15 represent the uncertainty of the calculated values for each condition, based on the standard deviation of the population of calculated values and the inherent uncertainty in the measurement.

Figure 14 shows the effect of chlorine injection on mercury removal, while firing PRB coal. The fact that removal before the baghouse decreases while removal across the baghouse increases is an interesting phenomenon, which puts emphasis on the complexity of the chlorine/mercury reaction chemistry present in coal-fired flue gas. More importantly, the total mercury removal only slightly increased, even though mercury oxidation was significant (see Fig. 6). This indicates that more than oxidation is necessary before high-calcium PRB ash will uptake mercury. Both Fig. 14 and Fig. 15 indicate that most of the Hg-removal occurred across the baghouse.

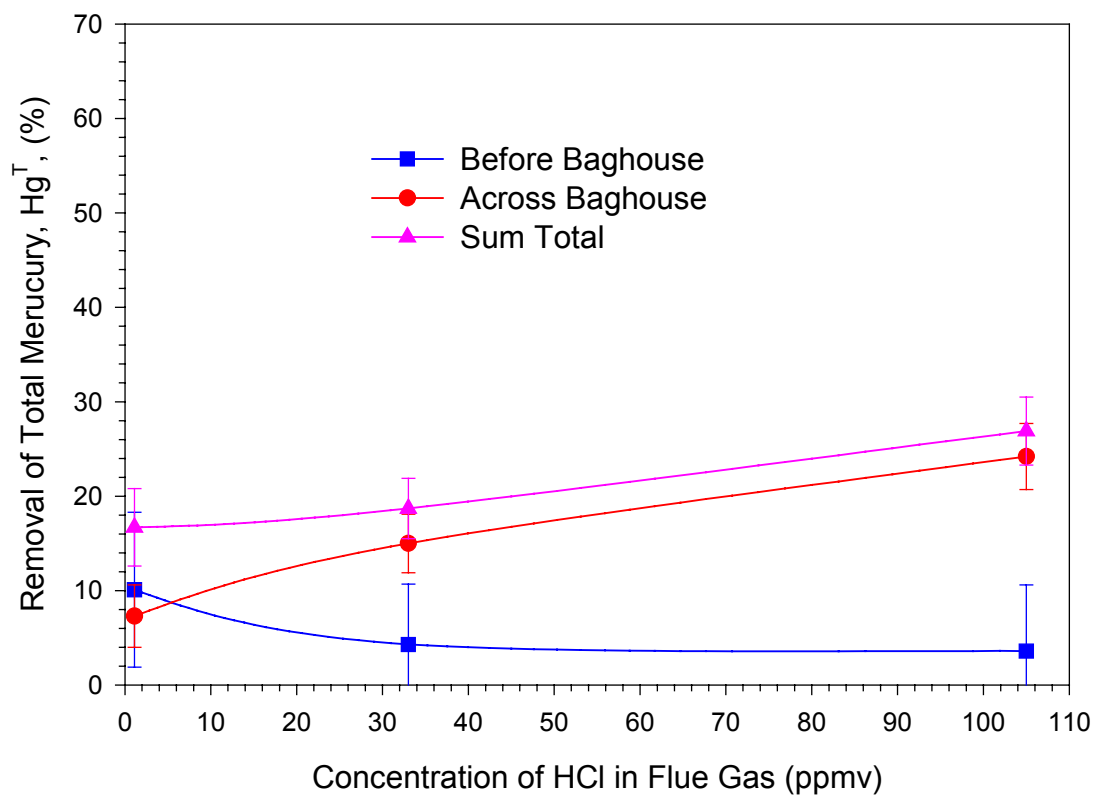


Figure 14. Total mercury removal while firing PRB coal and injecting Cl_2 through the burner.

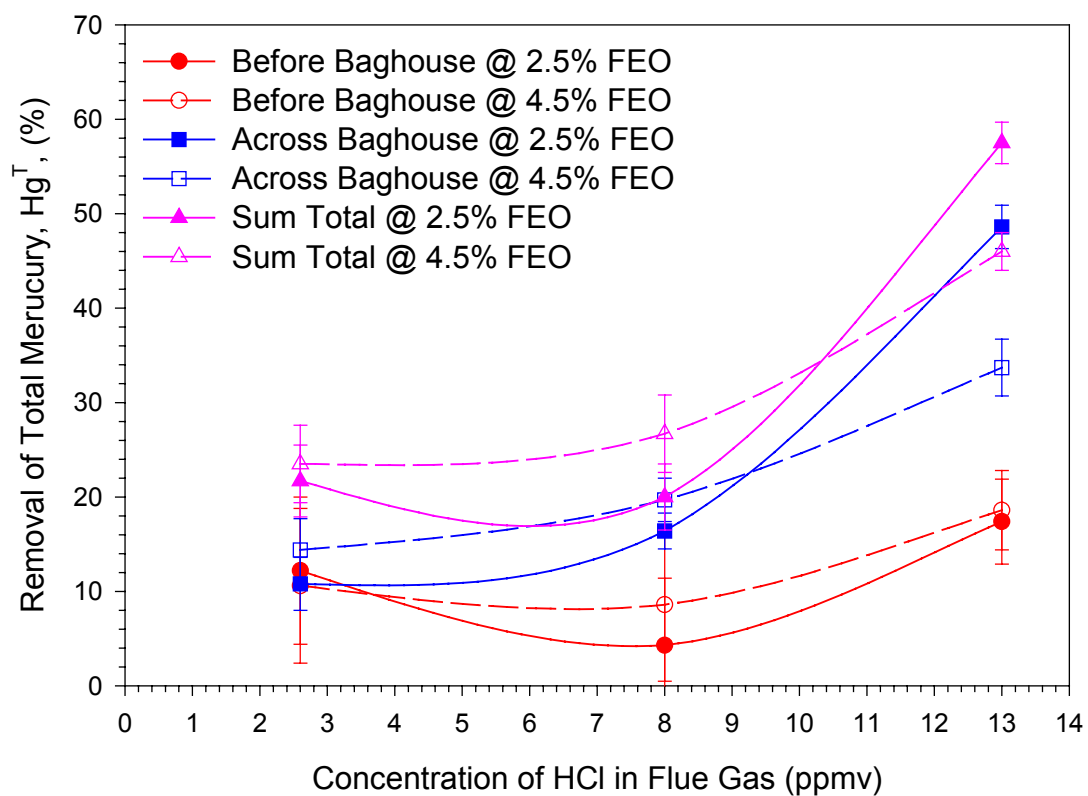


Figure 15. Total mercury removal as a function of flue-gas chlorine content for different coal blends at 2.5% and 4.5% FEO.

Figure 15 illustrates the extent of mercury removal as a function of flue-gas chlorine content for different blends of PRB and bituminous coal. Notice the difference in scale between Figs. 14 and 15. At 13 ppmv of HCl, the sum total of mercury removal is approximately 18% for PRB, while it is as much as 45% and 60% for the coal blends. Clearly, the other parameters associated with the bituminous coal are more important for Hg-removal than the difference in chlorine content. This is not surprising since the ash of bituminous coal was found to be a more important to Hg-oxidation than the total chlorine content (see Fig. 6). Hence, the increased oxidation of mercury for the coal blends may have significantly contributed to the increase in mercury capture.

Figure 16 presents measured removals of mercury before the baghouse for different coal blends at two different furnace exit oxygen (FEO) levels. A line representing removals for PRB-only at 3.5% FEO is included for reference. As shown (see Fig. 16), mercury removal before the baghouse for coal blends did not differ significantly from that measured for PRB only. In addition, the FEO level, which has an effect on unburned carbon (UBC) in the ash, did not have any significant impact for the conditions presented in Fig. 16.

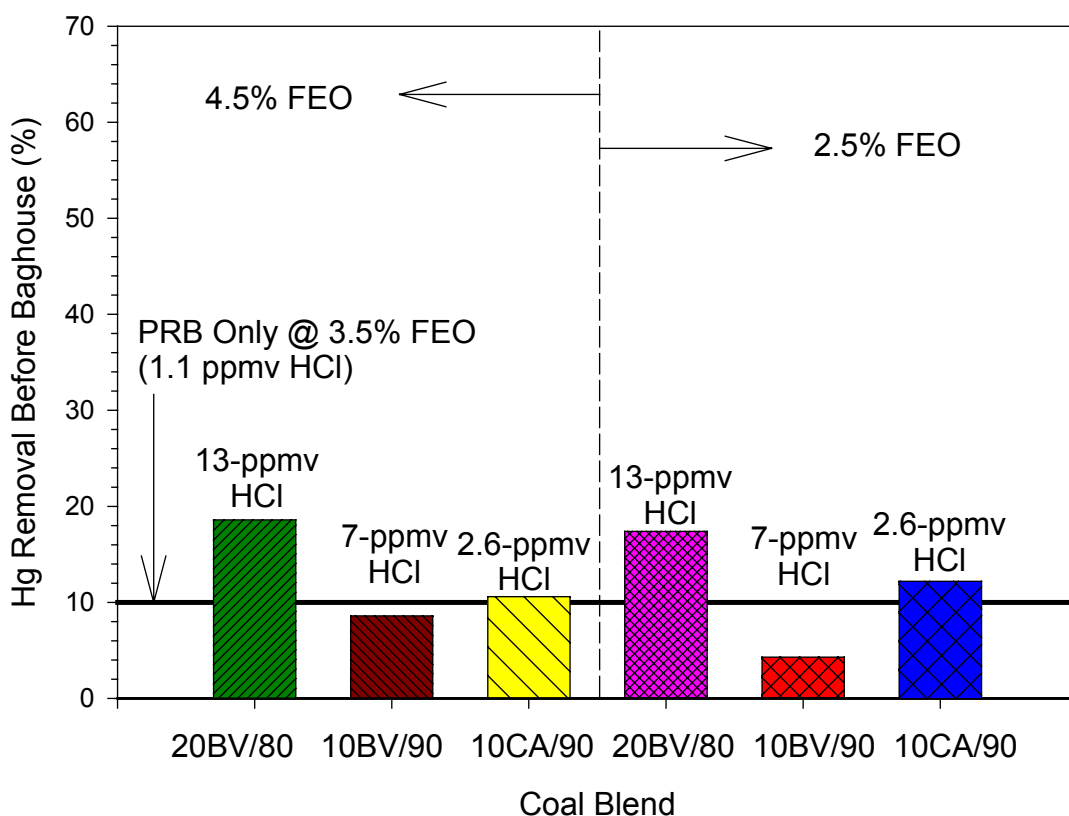


Figure 16. Mercury removal before the baghouse inlet for different blends of PRB and bituminous coal.

Figure 17 shows the sum total removal of mercury at the baghouse outlet for the same conditions presented in Fig. 16. Except for the vertical axis, Figs. 16 and 17 are similarly constructed. The sum total of mercury removal is greater for all coal blends than for PRB-only. However, the difference in removal magnitude is only significant for the 20% Blacksville/80% PRB blend (see Fig. 17). As shown, Hg-removals of nearly 60% were obtained for this blend, while only ~17% removal was observed while firing PRB coal only under similar conditions.

Figures 7 and 8 of the previous section indicate significantly more mercury oxidation at both the inlet and outlet of the baghouse for the coal blends than for PRB only. Mercury removals for the same coal blends (see Figs. 16 and 17) did not correspond with increased oxidation. Hence, while blending a small amount of bituminous coal with PRB coal can significantly increase mercury capture by the flyash, the effect of coal blending on Hg-capture is more than mere Hg-oxidation enhancement. As will be shown, the flyash produced from the coal blends has a *synergistic effect* on mercury capture beyond that of increasing mercury oxidation in the presence of high-calcium flyash.

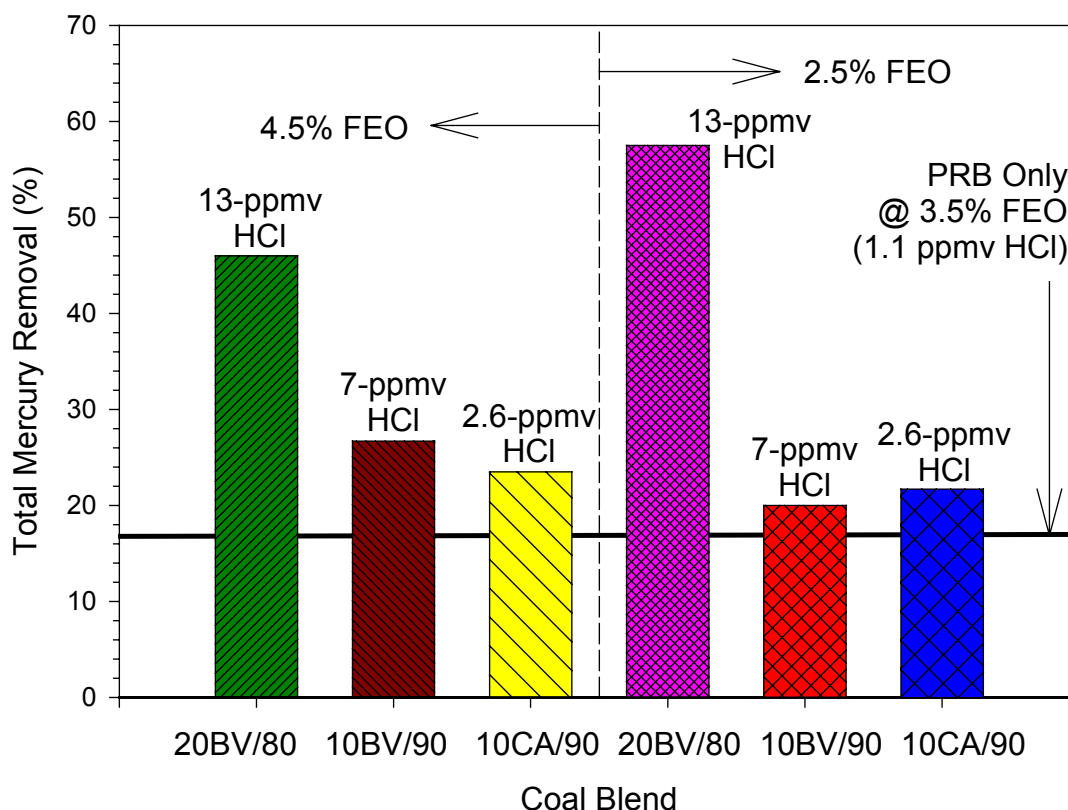


Figure 17. Total mercury removal at the baghouse outlet for different blends of PRB and bituminous coal.

Figure 18 illustrates the relationship of baghouse temperature with mercury removal, for the particular conditions of the SRI pulse-jet baghouse. The baghouse temperature was changed by adjusting the cooling rate in the final set of heat exchangers (see Fig. 3). Using this method to adjust baghouse temperature avoided the convoluting effect of changing moisture content. The small differences in mercury removal were obtained one after the other, by raising and subsequently lowering the baghouse temperature. For example, the low temperature condition was measured, followed by immediate change in heat extraction from the flue gas and rapid increase in baghouse temperature. An immediate change in mercury removal was observed and measured for several hours. Finally, heat extraction was altered to return to the low-temperature condition, and the mercury removal values returned to the low-temperature values previously measured. In this manner, errors associated with small operational differences from one run to another were eliminated.

Figure 18 illustrates the effect of temperature on the sum total of mercury removal for PRB-only and for 20% Blacksville coal blended with 80% PRB coal. Consistent with Fig. 9 in the previous section on Hg-oxidation, the coal blend is much more effective at removing mercury, and the relationship between capture and temperature is in the same direction as oxidation. Both Fig. 9 and Fig. 18 suggest that different governing mechanisms are controlling mercury speciation (including capture) for the coal blend than are controlling for PRB-only. The behavior of the coal blend with temperature is in the opposite direction from PRB-only, for the conditions in the pulse-jet baghouse. Furthermore, Fig. 18 (and Fig. 9) suggests that coal blending not only improves mercury capture directly, but may also change the governing mechanisms such that low-temperature capture technologies are more effective for oxidizing and capturing mercury. For PRB-only, higher temperatures were more effective for the particular conditions within the pulse-jet baghouse investigated.

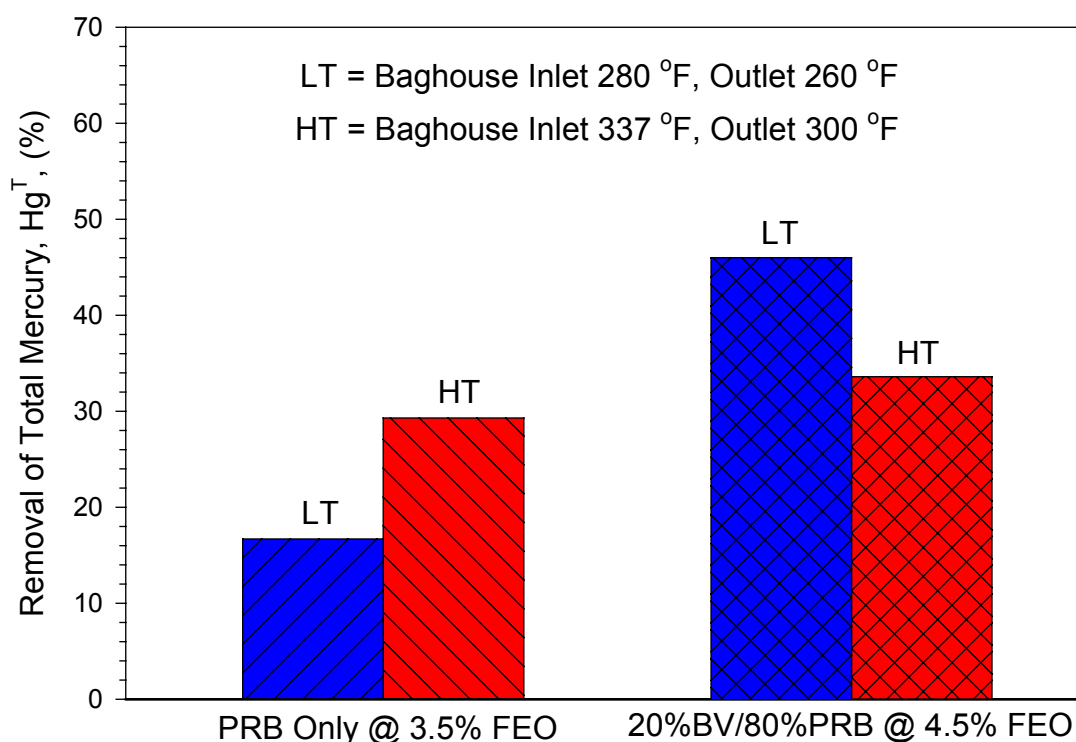


Figure 18. Effect of temperature on the sum total of mercury removal (Hg^T).

Figure 19 allows examination of the relationship between SO_2 and the sum total of mercury removal. It does not appear (see Fig. 19) that there is a direct relationship between SO_2 and mercury capture. Some correlation is apparent, perhaps only because SO_2 increases with increasing bituminous coal in the blend. The effect of SO_2 on Hg-oxidation and capture by flyash will be examined further in subsequent tests by isolating this parameter.

The effect of UBC and ash minerals on the sum total of mercury removal is presented in Fig. 20. As shown, both UBC and the Fe_2O_3/CaO ratio in the ash correlate directly with mercury removal. A linear curve fit with a non-zero y-intercept fits the UBC data best, while an exponential rise to maximum, which passes through the origin, fits the data correlation with the iron to calcium ratio best.

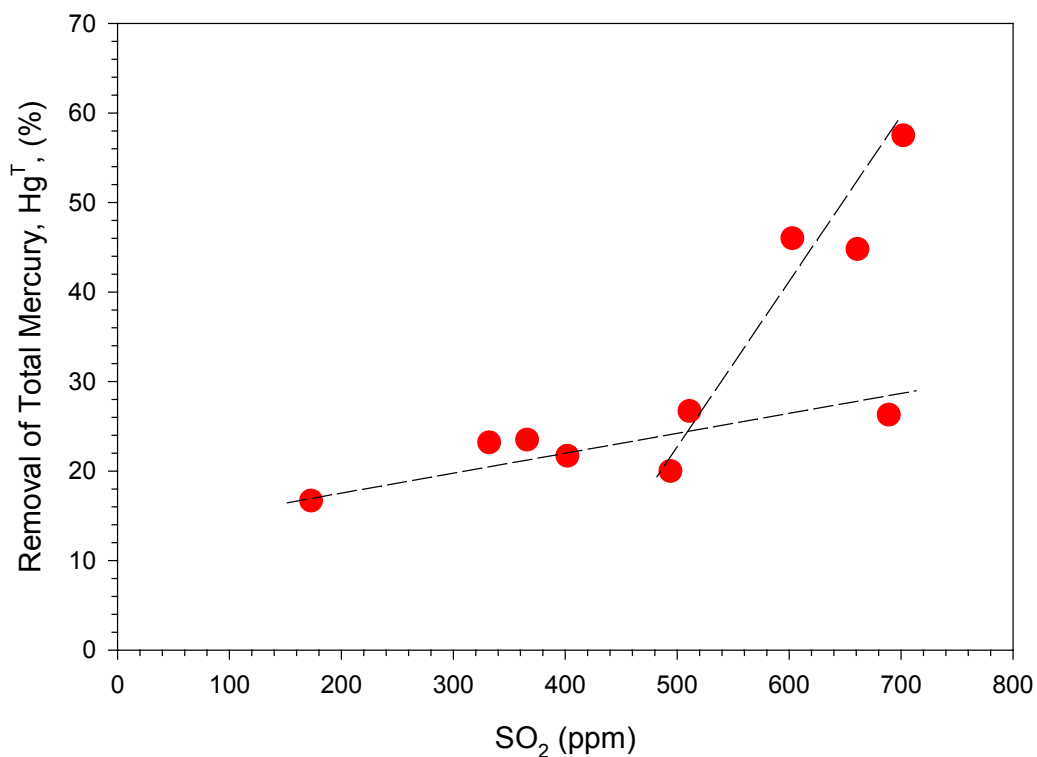


Figure 19. Effect of SO_2 on the sum total of mercury removal.

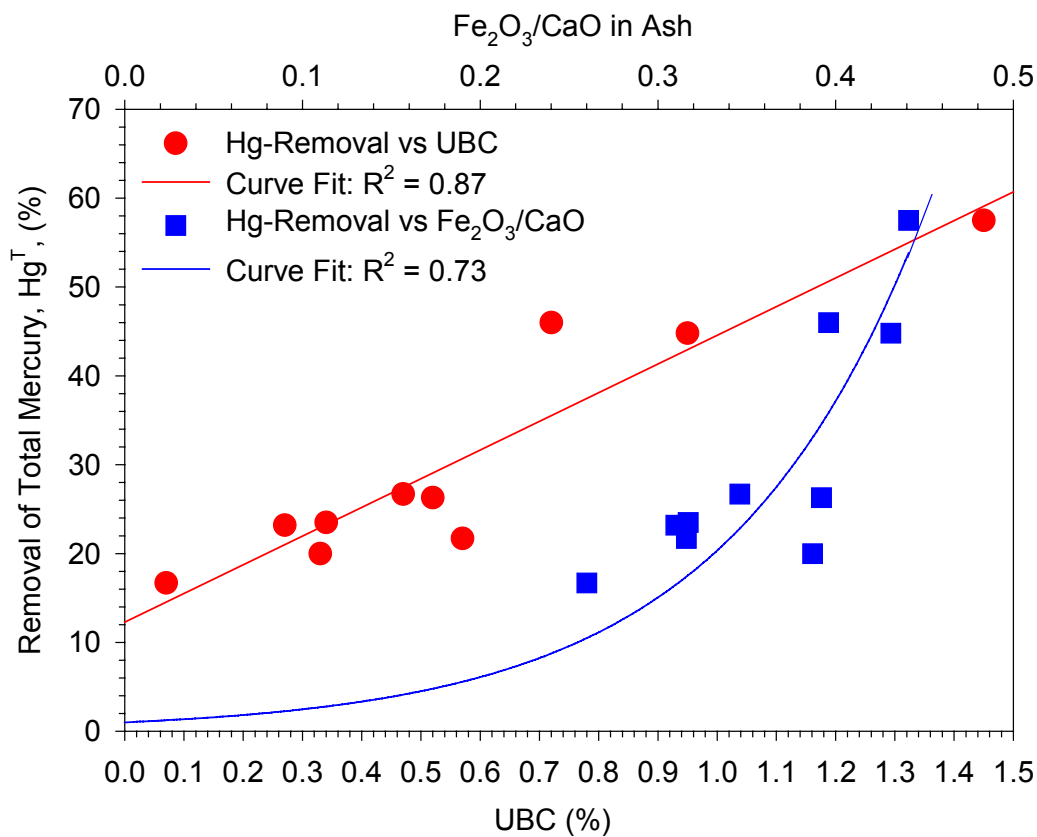


Figure 20. Effect of UBC and ash minerals on the sum total of mercury removal.

Further tests are necessary in order to separate the individual contribution of UBC, iron, or other minerals to the capture of mercury by flyash. However, it has been shown that flyash composition is the most important factor in determining the impact of blending bituminous coal with PRB coal to increase mercury uptake by the flyash. This fact is further emphasized in Fig.21.

Figure 21 contains the results of the baghouse ash injection tests conducted at the high-temperature (337 °F to 300 °F) baghouse condition, which is most favorable for mercury removal by PRB flyash and least favorable for the coal blends (see Fig.18). The baseline case of PRB-only was compared with three different baghouse injection conditions, 100% Choctaw ash, and two blends of Choctaw ash with hydrated lime, 20% Choctaw ash/80% hydrated lime and 50% Choctaw ash/50% hydrated lime. Particulate was injected into the baghouse at a rate approximately equal to the mass rate of flyash flowing into the baghouse from the furnace. The baghouse was pulsed down at the beginning of each new injection condition, to avoid excessive buildup of material or long transition times from a previous condition. Approximately the same mass rate of particulate was used for each baghouse injection condition.

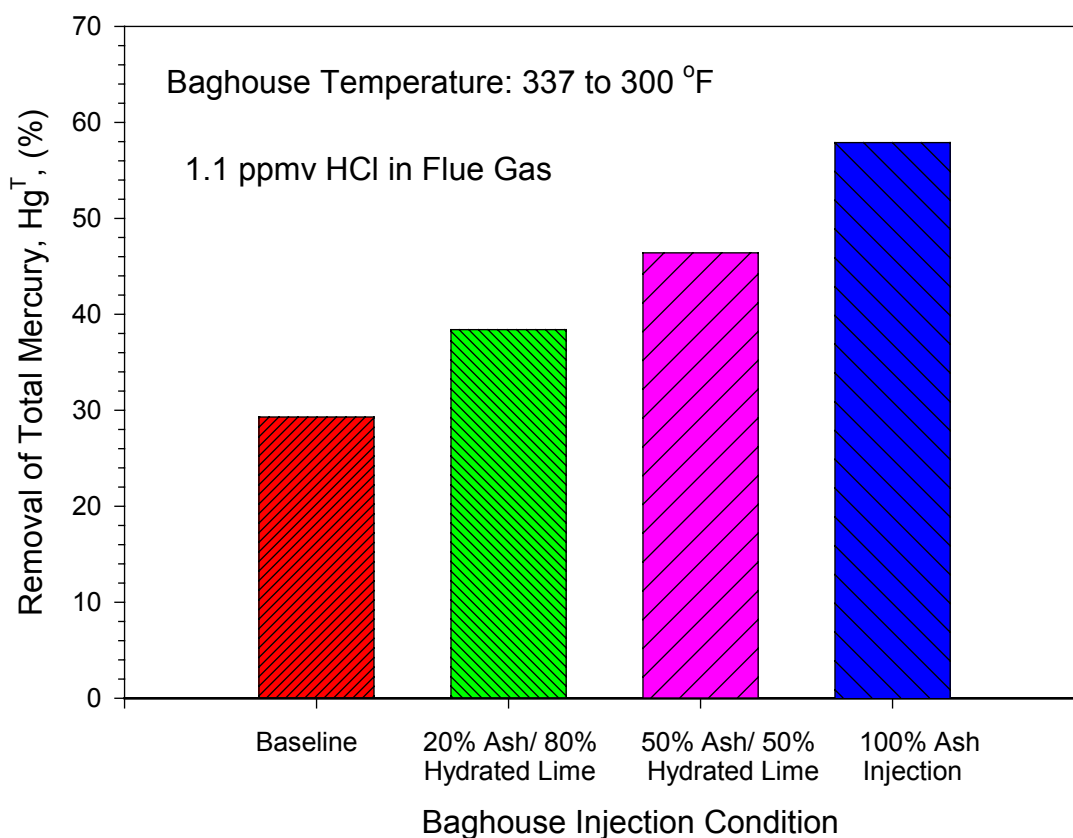


Figure 21. Sum total of mercury removal from injecting Choctaw America coal ash and hydrated lime into the baghouse while burning PRB coal.

Hydrated lime has a surface area ($\sim 18 \text{ m}^2/\text{g}$) much greater than that of Choctaw ash (see Table 8). Therefore, the influence of ash composition could be distinguished from the mere increase in mass loading or surface area. As shown in Fig. 21, the injection of 100% Choctaw ash significantly enhanced the sum total of mercury removal. Additional hydrated lime injection was relatively benign in its effect on Hg-removal. As illustrated in Fig. 21, Hg-removal

increased with increasing concentration of Choctaw ash. The hydrated lime acted merely to dilute the impact of injecting Choctaw ash. Apparently, the catalytic properties of the high-iron ash were not only important in the oxidation of mercury (see Fig. 13) but also in enhancing the capture of mercury as well. A comparison of Fig. 13 and Fig. 21 reveals that the extent of enhanced mercury removal is greater than the extent of oxidation enhancement, although extensive Hg-oxidation occurred for all conditions. It is likely that the bituminous ash iron and UBC were important catalytic components that promoted mercury removal in the baghouse.

The high-temperature baghouse condition, used for the direct ash-injection tests was more favorable for baseline (PRB only) Hg-removal (see Fig. 18). However, the low-temperature condition was more favorable for enhancement of Hg-removal by the coal blends (see Fig. 18). Therefore, the impact of direct ash injection on Hg-removal at the lower temperature condition would likely be more dramatic.

Figure 22 illustrates the effect of hydrated lime injection on mercury removal when flue-gas mercury was highly oxidized, which high-oxidation was achieved by blending 10% Blacksville with 90% PRB coal by mass.

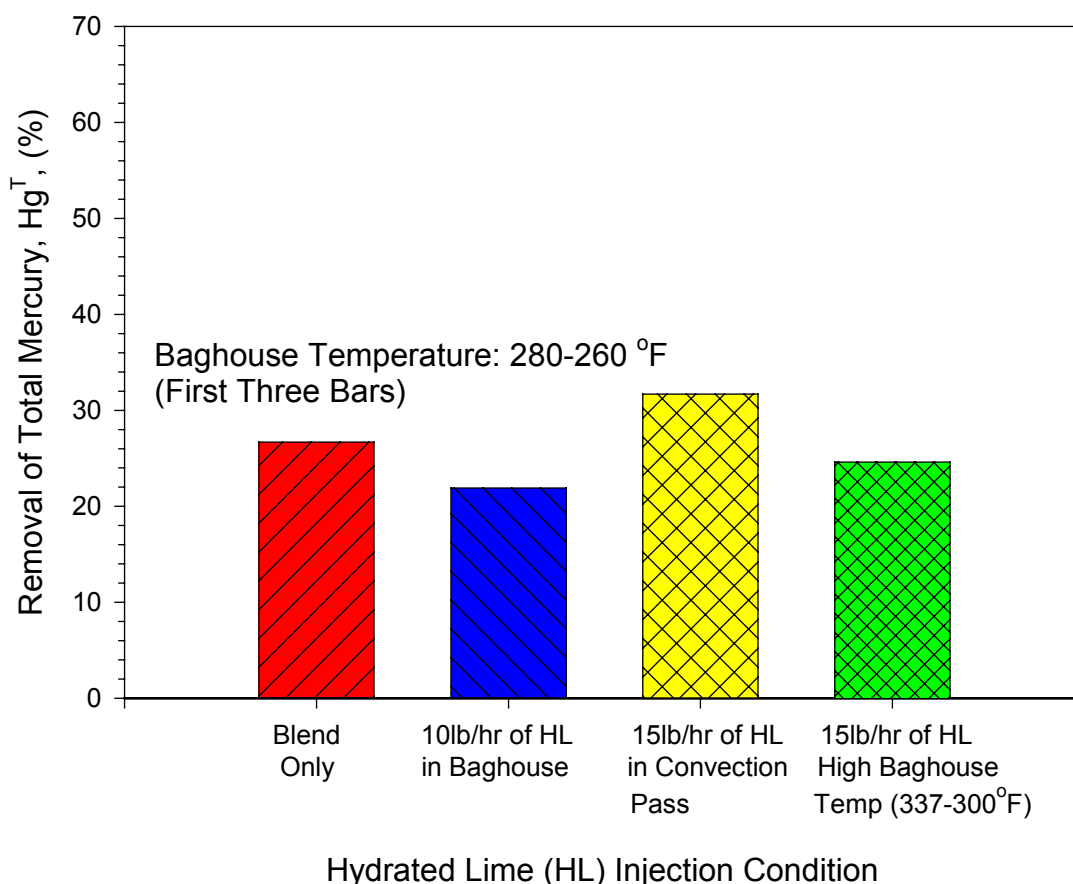


Figure 22. Effect of hydrated lime injection on the sum total of mercury removal when flue-gas mercury was highly oxidized, achieved by blending 10% Blacksville coal with 90% PRB.

Although the mercury was highly oxidized (see Fig. 23) at the baghouse outlet, the injection of hydrated lime did little to improve the sum total of mercury removal. Several different hydrated lime (HL) injection strategies were evaluated, including direct injection of HL into the baghouse, injection well upstream where flash-calcination can help increase the sorbent

surface area, and injection upstream of the baghouse with an increased baghouse temperature. The results from these different HL injection conditions are shown in Fig. 22. As shown there is little difference in mercury removal between conditions. Injection of hydrated lime has been shown to effectively increase capture of mercury across a baghouse while burning bituminous coal with a high fraction of oxidized mercury [12]. However, in this case hydrated lime injection did not significantly increase mercury removal for the coal blend with highly oxidized mercury. This indicates that other parameters are important for Hg-capture by HL (and perhaps calcium in general) than the fraction of mercury oxidized.

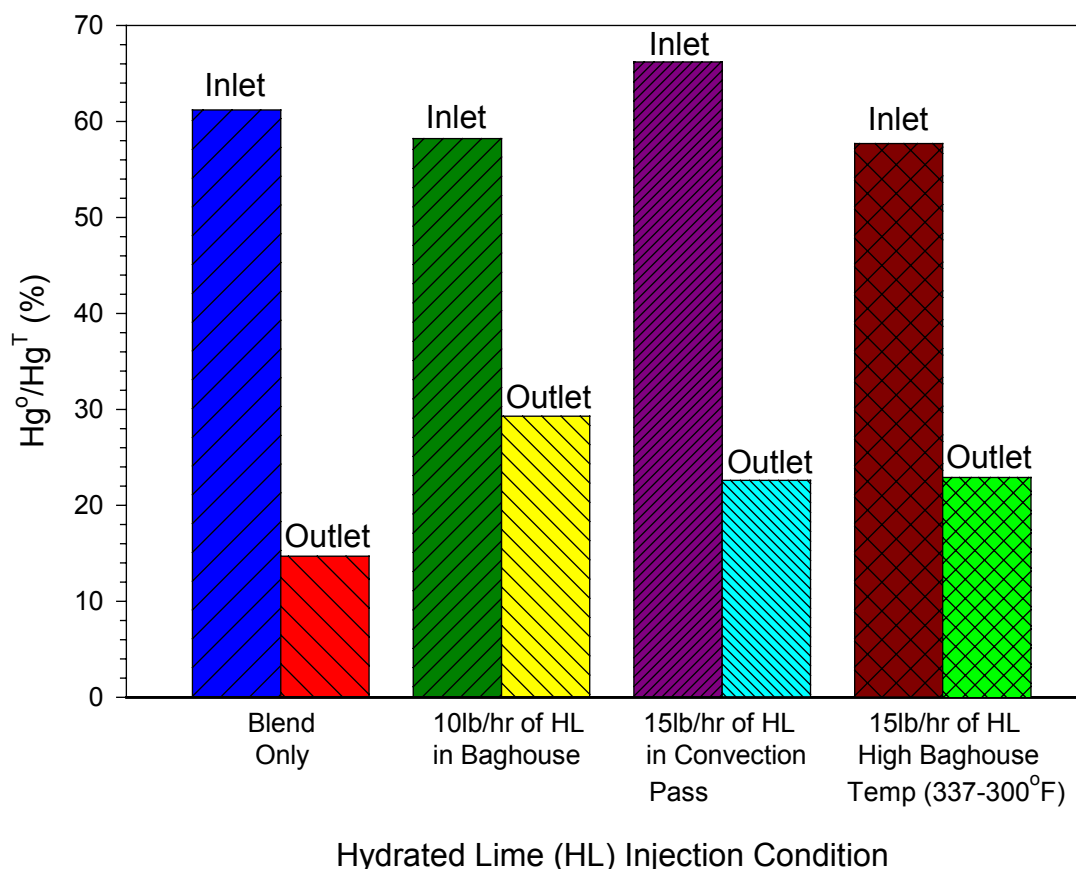


Figure 23. Fraction of elemental mercury measured at the inlet and outlet of the baghouse during hydrated lime injection.

Figure 24 illustrates the effectiveness of mercury capture enhancement by hydrated lime injection while burning Choctaw America, a low-chlorine bituminous coal. The 15 lb/hr of HL injected was approximately half the flyash loading. As shown in Fig. 24, the injection of HL upstream of the baghouse increased the sum total of mercury removal from ~25% to ~80%. This change in removal occurred while the fractions of mercury oxidized did not change significantly at either the inlet or outlet of the baghouse. Apparently, the capture of oxidized-mercury by calcium, either in hydrated lime or PRB flyash, is catalytically enhanced by the presence of bituminous ash material (i.e., UBC and/or iron). This enhancement of capture is more than an enhancement of oxidation. It is also an enhancement of the capture reaction itself.

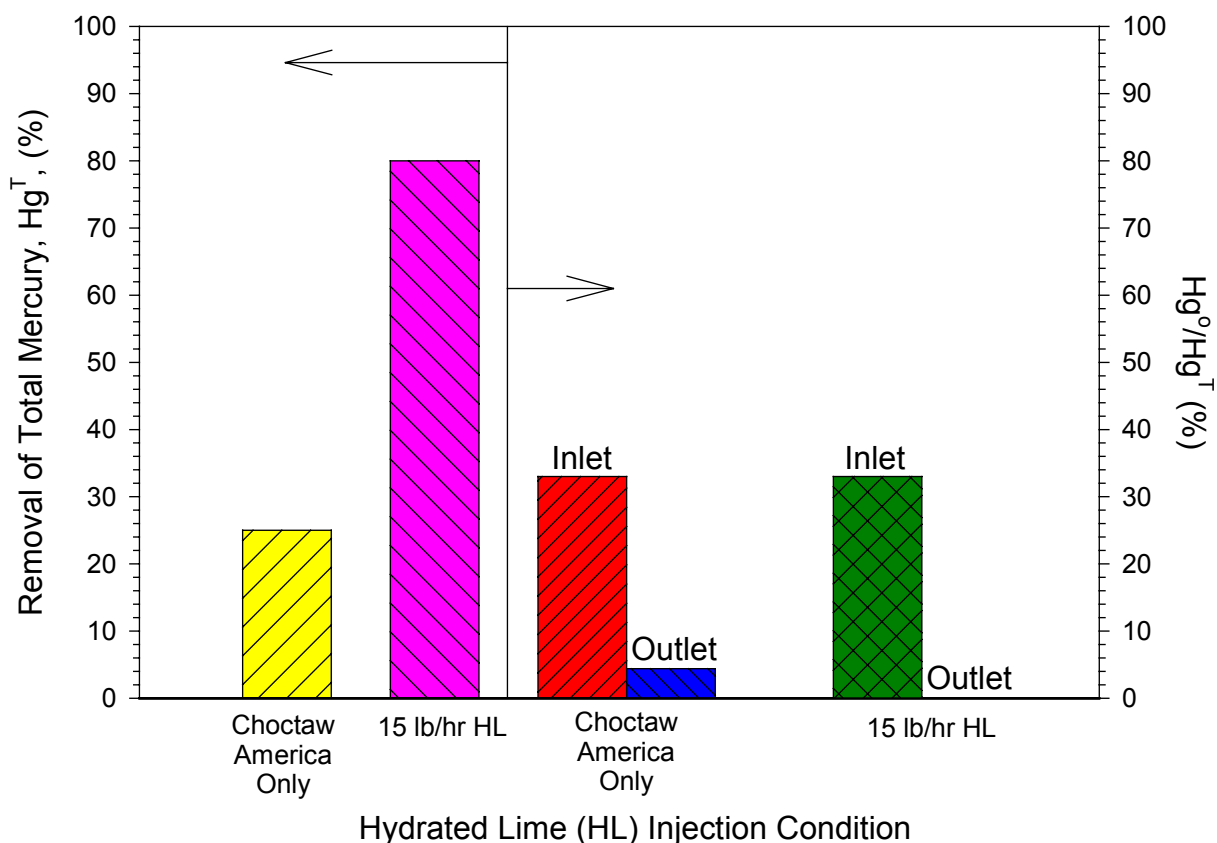


Figure 24. Effect of hydrated lime injection on the sum total of Hg-removal, while firing Choctaw America coal at the low baghouse-temperature condition (280-260 °F).

Summary of Mercury Capture Section

Total chlorine content, injected independently through the burner or inherent in the coal, had little effect on total mercury removal. In terms of differences observed between PRB sub-bituminous coals and bituminous coals in full-scale boilers, catalytic enhancement by fly ash is a much more important factor in mercury removal (not just oxidation) than flue-gas total chlorine content. PRB-ash itself captures some mercury across the baghouse, which capture was enhanced significantly (~45%) with small increases in temperature (~Δ40 °F). A synergistic relationship was observed in this investigation between PRB ash and bituminous ash. Not only did the presence of bituminous ash catalyze Hg-oxidation, the mixture of PRB and bituminous ash was much more effective at capturing oxidized mercury (i.e., HgCl_2) than either PRB or bituminous ash alone. It is believed that bituminous ash catalyzed both the reaction of Hg^0 with HCl to form HgCl_2 (see Equ. 1 and 2) and the reaction of HgCl_2 with Calcium (i.e., Ca, CaO, $\text{Ca}(\text{OH})_2$, etc.) to form particulate bound mercury. It may be that bituminous ash catalyzes the direct reaction of Hg^0 with CaO to form particulate bound mercury as well. Both UBC and iron are potential catalytic materials of importance in bituminous ash. The catalytic activity and availability of iron may be important and may differ between coal types.

These results suggest that coal blending may play an important role in mercury mitigation strategies of the future, but substantially more data are needed to confirm this hypothesis and understand the governing processes well enough to rely on such an approach as a compliance

strategy. In this pilot combustor, injection of low-UBC (between 3 and 4%) bituminous ash into the baghouse resulted in mercury removals of 60%. In addition, injection of hydrated lime into the baghouse while burning a low-chlorine bituminous coal resulted in mercury removals of ~80%. Finally, mercury removal decreased with decreasing temperature while burning PRB coal-only but increased with decreasing temperature while burning blends of PRB and bituminous coals (10 or 20% bituminous by mass). Hence, coal blending may increase the favorability of low-temperature mercury removal for power plants primarily burning PRB coal.

Conclusions

The focus of this work was on Powder River Basin (PRB) sub-bituminous coals and bituminous coals with low unburned carbon (UBC) levels. All of the conclusions presented apply to high-efficiency low-UBC combustion conditions.

1. The catalytic material in coal ash is a more important factor in determining mercury oxidation and capture than the total flue-gas chlorine content.
2. There is a *synergistic effect* of ash mixtures resulting from PRB sub-bituminous and bituminous coal blending. Significantly more mercury was captured by a blend of PRB ash with a small amount of bituminous ash than was captured by either PRB or bituminous ash alone.
3. Bituminous ash not only catalytically enhances mercury oxidation, it catalytically enhances the capture of oxidized mercury by calcium particulate matter (i.e., PRB ash and hydrated lime).
4. The primary parameters responsible for enhancement of mercury oxidation and capture for blends of PRB and bituminous coal are UBC and mineral matter (i.e., iron) in bituminous ash. The form and availability of iron may be significant, which may be distinctly different for PRB and bituminous coal ash. Further tests will be performed to ascertain the relative importance of UBC and iron to the catalytic enhancement of mercury oxidation and capture.
5. Mercury oxidation and capture was found to increase with decreasing temperature (i.e., from 300 to 260 °F at the baghouse outlet) for 10% Blacksville bituminous coal blended with 90% PRB coal. The opposite was found for PRB-only. Mercury mitigation by temperature reduction (i.e., in the particulate control device) may be much more effective for power plants that primarily burn PRB coal if they blend with a small amount of bituminous coal.
6. Hydrated lime may be an effective sorbent for mercury removal, provided it is mixed with catalytic material, such as that found in bituminous ash (UBC < 4%).
7. Direct injection of bituminous ash into the flue gas or baghouse while firing PRB coal, may be an effective means of capturing mercury in the flyash. No chlorine injection or other additional attempts to oxidize the mercury were necessary in this work.

Future Work

Sodium Tetrasulfide

In the next quarter, Southern Research Institute will investigate another promising mercury mitigation technology that has been proven successful for waste incineration units. Sodium tetrasulfide has been successful at capturing total mercury from waste incinerators, when

injected ahead of a dry scrubbing unit containing calcium-based sorbents [19]. Sodium tetrasulfide sprayed into the duct ahead of a dry scrubber, forms dispersed tiny droplets in the flue gas. These dispersed droplets then react with both elemental and oxidized mercury to form mercuric sulfide, a non-poisonous stable compound. The reactions are as follows:



Sodium tetrasulfide injection has been shown to be effective at capturing mercury from full-scale incinerator units. It has not, however, been tested in coal-fired flue gas. Coal-fired flue gas contains a lower concentration of mercury and acid gases than does flue gas derived from incineration.

Injection of sodium tetrasulfide into flue gas results in the formation of H_2S , which is an essential part of the capture reaction (see Equ. 1 above). However, H_2S is also a pollutant that must be controlled. Consequently, injecting sodium tetrasulfide (Na_2S_4) just ahead of a dry scrubbing unit will potentially remove all H_2S and SO_3 inherent in the coal-derived flue gas as well as that created by the injection of Na_2S_4 . This technical approach to mercury emission mitigation is a logical combination of additive with calcium-based sorbents.

Babcock Power Inc. has extensive expertise with Na_2S_4 injection for mercury control in waste incinerators. A test of Na_2S_4 injection for mercury control in coal-fired power plants is scheduled tentatively for the third week in April. Babcock Power Inc. has agreed to supply equipment, personnel, and expertise for this test in the CRF, all of which will be contributed as cost share to the project.

The April test will be conducted using the Fluidized Bed Desulfurization Reactor (FBDR) in once through mode. Sodium tetrasulfide will be injected with a heated air-atomizing nozzle in the center of the duct at the beginning of the U-tube section of the FBDR (see Appendix A) to allow a long stretch of duct for the finely atomized spray to evaporate and decompose. Simultaneous injection of calcium-based sorbents will be investigated to determine any synergistic interactions.

ADVACATE Sorbent Multi-Pollutant Control

In 1993, Southern Research Institute (SRI) tested a sorbent known as ADVACATE, a high surface area sorbent derived from hydrated lime slurried with fly ash to enhance its ability to capture acid gases, particularly SO_x [20-25]. During the test at Southern Research Institute, ADVACATE sorbent was tested for its ability to capture SO_2 and total mercury across a baghouse with spray cooling [20]. The ADVACATE sorbent was demonstrated to capture 80% of the sulfur and 99+% of the total mercury (by a mercury-in-ash mass balance) by the baghouse outlet, while burning Old Ben, a high-volatile bituminous coal [20]. While the data taken in that investigation is limited in terms of mercury measurements, it does indicate promise for ADVACATE sorbent to simultaneously capture SO_2 and mercury. The fact that ADVACATE sorbent is derived from coal ash suggests that it may have desirable catalytic properties as well as sorptive capabilities. This is particularly interesting in light of the results presented in this report on the impact of UBC and other ash minerals on mercury oxidation and capture. Consequently, ADVACATE sorbent will be tested while firing PRB coal, via baghouse injection and also

possibly in a semi-dry scrubbing system, such as in the Fluidized Bed Desulfurization Reactor (FBDR) at Southern Research Institute (SRI). Dry scrubbing using ADVACATE sorbent is a potential multi-pollutant control strategy for SO₂, SO₃ and mercury.

Through EPA's research agreements with various universities and research institutions, ADVACATE sorbent technology has evolved into a simple add-on technology easily retrofit onto existing utility boilers with minimal disruption [22]. Because the ADVACATE process uses coal fly-ash to slurry with calcium hydroxide, material handling costs are low and the cost of sorbent will be much lower than for activated carbon [11]. The cost of hydrated lime is approximately 10 times less than commercial activated carbon. In addition, the disposal costs will be much less as well. The used sorbent/ash product may even be sold as a valuable byproduct for the cement industry or used for road fill. Appropriate leaching and stability tests will need to be performed on the sorbent/ash products.

Since there are no current production facilities making ADVACATE sorbent, the cost of producing the ADVACATE sorbent in the laboratory for testing is much higher than the actual cost of the sorbent once the technology is implemented.

Isolating UBC and Ash Minerals

As a follow on to the work presented in the present report, the impacts of unburned carbon (UBC) and ash minerals (particularly iron) on mercury speciation will be investigated. Initially these parameters will be isolated to evaluate the impact of each parameter on Hg-speciation independent of other interactions. First, PRB coal will be fired under combustion conditions that produce high UBC (primarily unburned char), without the creation of much soot. This will effectively isolate the impact of UBC from other parameters associated with bituminous coal ash minerals. Furthermore, PRB has a low chlorine content and sulfur content, which can be increased independently in the flue gas by doping as desired, thus isolating the impact of each parameter and the interactions between each parameter. The results of this test will either show that UBC dominates the catalytic behavior of bituminous ash for both Hg-oxidation and capture or it will reveal that minerals in bituminous ash also play a significant role. The investigation will lead to quantitative measurement of the impact of each respective parameter and their interactions.

SO₂ will also be isolated for its impact on Hg-speciation, although the belief from the investigation thus far is that total SO₂ concentration has little impact on Hg-speciation.

This investigation of ash-chemistry details will provide information that will make it possible to directly design effective calcium-based sorbents and technology strategies for mercury mitigation with a high degree of success. For example, for a plant producing a high-calcium ash with low UBC, it may be necessary to inject catalytic material such as that found in bituminous ash. On the other hand, it may be necessary to inject only hydrated lime in a plant burning bituminous coal. Furthermore, the development of advanced sorbents such as ADVACATE will prosper from the knowledge gained on catalytic and synergistic ash-composition effects on Hg-oxidation and capture.

References

1. Gale, T. K., "Mercury Control with Calcium-Based Sorbents and Oxidizing Agents" Quarterly Report – DE-PS26-02NT41183 for period Oct. 1st through Dec. 31st, 2002.
2. Senior, C. L., Chen, Z., and Sarofim, A. F., "Mercury Oxidation in Coal-Fired Utility Boilers: Validation of Gas-Phase Kinetic Models", *A&WMA 95th Annual. Conference.*, Baltimore MD, (2002).
3. Niksa, S., Helble, J. J., Fujiwara, N., "Kinetic Modeling of Homogeneous Mercury Oxidation: the importance of NO and H₂O in predicting oxidation in coal-derived systems", *Environ. Sci. Technol.*, **35**: 3701-3706 (2001).
4. Niksa, S., Fujiwara, N., Fujita, Y., Tomura, K., Moritomi, H., Tuji, T., and Takasu, S., "A Mechanism for Mercury Oxidation in Coal-Derived Exhausts" *J. A&WMA* **52**: 894-901 (2001).
5. Chen, Z., Senior, C. L., and Sarofim, A. F., "Modeling of Mercury States in Coal-Fired Utility Boilers" *27th Annual Technical Conference on Coal Utilization and Fuel Systems*, Clearwater Florida, March 4-7 (2002).
6. Niksa, S. and Helble, J. J., "Interpreting Laboratory Test Data on Homogeneous Mercury Oxidation in Coal-Derived Exhausts" *Fuel*, Submitted, 2002.
7. Lee, C. W., Kilgroe, J. D., and Ghorishi, S. B., "Speciation of Mercury in the Presence of Coal and Waste Combustion Fly Ashes", *A&WMA's 93rd Annual Conference and Exhibition*, Salt Lake City, UT (2000).
8. Niksa, S. and Fujiwara, N., "Predicting Mercury Speciation in Coal-Derived Flue Gases", *EPRI-DOE-EPA-A&WMA Combined Utility Air Pollution Control Symposium: The MEGA Symposium*, May (2003).
9. Sliger, R. N., Kramlich, J. C., Marinov, N. M., "Towards the Development of a Model for the Homogeneous Oxidation of Mercury by Chlorine Species", *Fuel Process. Technol.*, **65-66**(0): 423-438 (2000).
10. Norton, G. A., "Effects of Fly Ash on Mercury Oxidation During Post Combustion Conditions", Annual Report – DE-FG26-98FT40111 for period Sept 1st, 1999 through Aug. 31st, 2000.
11. Ghorishi, S. B. and Sedman, C. B., "Combined Mercury and Sulfur Oxides Control Using Calcium-Based Sorbents" *EPRI-DOE-EPA Combined Utility Air Pollutant Control Symposium*, Washington, DC (1997).
12. Gale, T. K., "Mercury Control with Calcium-Based Sorbents and Oxidizing Agents" Topical Report-DE-FC26-01NT41183 for period Sept. 5th 2001 through May 31st 2002.

13. Weilert, C. V. and Randall, D. W., "Analysis of ICR Data for Mercury Removal from Wet and Dry FGD", *EPRI-DOE-EPA Combined Utility Air Pollution Control Symposium: The MEGA Symposium*, August 20-23 (2001).
14. Behrens, G., "Final Report: An Assessment of Mercury Emissions from U. S. Coal-Fired Power Plants", No.1000608, EPRI, Palo Alto, CA (2000).
15. Blythe, G. M. and Richardson, C. F., "Catalytic Oxidation of Mercury in Flue Gas for Enhanced Removal in Wet FGD Systems" *EPRI-DOE-EPA Combined Utility Air Pollution Control Symposium: The MEGA Symposium*, August 20-23 (2001).
16. Ghorishi, S. B., Singer, C. F., Jozewicz, W. S., Sedman, C. B., and Srivastava, R. K., "Simultaneous Control of Hg⁰, SO₂, and NO_x by Novel Oxidized Calcium-Based Sorbents" *J. Air & Waste Manage. Assoc.* **52**:273-278 (2002).
17. Ghorishi, S. B., Keeney, R. M., Serre, S. D., Gullett, B. K., and Jozewicz, W. S., *Environ. Sci. Technol.* **36**: 4454-4459 (2002).
18. Starns, T., Bustard, J., Durham, M., Lindsey, C., Martin, C., Schlager, R., Donnelly, B., Sjoström, S., Harrington, P., Haythornthwaite, S., Johnson, R., Morris, E., Chang, R., and Renninger, S., "Full-Scale Test of Mercury Control with Sorbent Injection and an ESP at Wisconsin Electric's Pleasant Prairie Power Plant", *A&WMA 95th Annual. Conference*, Baltimore MD, (2002).
19. Licit, A., Schuttenhelm, W., and Klein, M., "Mercury Control for MWC's Using The Sodium Tetrasulfide Process", *In Press* (2002).
20. Gooch, J. P., Marchant Jr., G. H., Monroe, L. S., "Integrated Control Systems for Particulate and Acid Gases" *Draft Report to S.L. Rakes, EPA Project Officer* (1993).
21. Jozewicz, W. and Rochelle, G. T., "Fly Ash Recycle in Dry Scrubbing" *Environ. Progress*, **5**: 219 (1986).
22. Jozewicz, W., Hall, B. W., Singer, C., and Sedman, C. B., "ADVACATE—Low-Cost Process for SO₂ Control", *Intern. Symp. on Environ. Contamination in Central and Eastern Europe*, Budapest, Hungary, October 12-16 (1992).
23. Sedman, C. B., Maxwell, M. A., Jozewicz, W., and Chang, J. C. S., "Commercial Development of the ADVACATE Process for Flue Gas Desulfurization", *25th IECEC*, Reno NV, August (1990).
24. Jozewicz, W., Chang, J. C. S., Sedman, C. B., and Brna, T. G., "Silica-Enhanced Sorbents for Dry Injection Removal of SO₂ from Flue Gas" *JAPCA* **38**: 1027-1034 (1988).

25. Hall, B. W., Singer, C., Jozewicz, W., Sedman, C. B., and Maxwell, M. A., "Current Status of the ADVACATE Process for Flue Gas Desulfurization", *AWMA J.*, **42**: 103-110 (1992).

APPENDIX A

EXPANDED EXPERIMENTAL

The Combustion Research Facility (CRF) at Southern Research Institute (SRI) was fired at 1.0 MW thermal or about 0.35 MW electric. The design of the facility was carefully chosen to provide a close simulation of the physical processes that occur in a full-scale utility boiler. The facility, shown in Fig.A1, consists of a coal crushing and milling area, a coal feeding system, a vertical refractory lined furnace, a single up-fired burner, a horizontal convective section pass with air-cooled tube banks, a series of heat exchangers, an electrostatic precipitator, a pulse jet baghouse, and a packed column scrubber.

SOUTHERN RESEARCH COMBUSTION RESEARCH FACILITY

Birmingham, AL

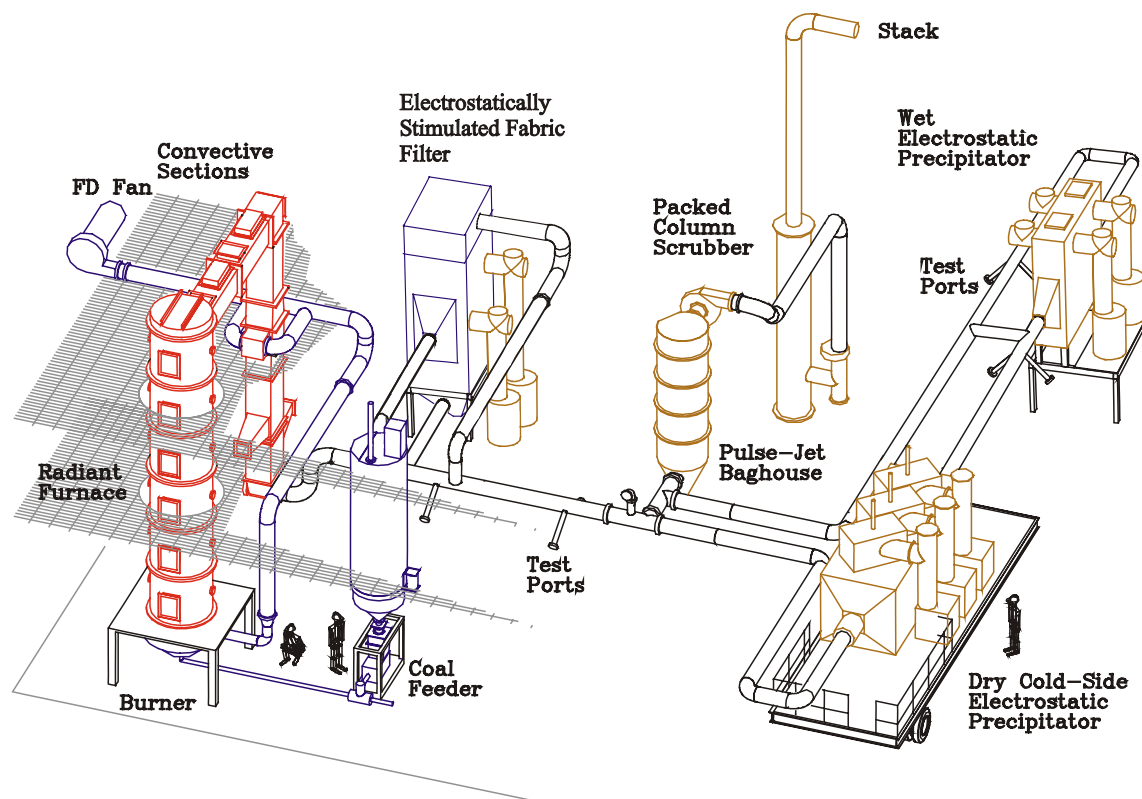


Figure A1. The Southern Company / Southern Research Institute Combustion Research Facility.

Fuel Preparation

The fuel preparation area includes an open area storage yard, covered on-site storage bins, a rotary drum coal crusher, a CE Raymond bowl mill, and pulverized coal storage. The coal mill is a refurbished and instrumented Model 352 CE-Raymond bowl mill, which has a rated capacity of 2 tons per hour. This type of mill should give representative milling simulations of the different air-swept table and roller mills normally used in power plant service.

Temperature/Time History Comparison

The temperature/time history within the Combustion Research Facility (CRF) is consistent with that of full-scale boilers, from the burner all the way through the economizer. Figure A2 shows a comparison of the CRF temperature profile with that of various Southern Company full-scale facilities.

Radiant Furnace

The furnace is a vertical, up-fired, 28-foot high cylinder, with an inner diameter of 3.5-feet (see Figure A1). This allows gas velocities of 10 to 20-feet per second and residence times of 1.3 to 2.5 seconds, depending upon the firing rate. The design furnace exit gas temperature is 2200°F.

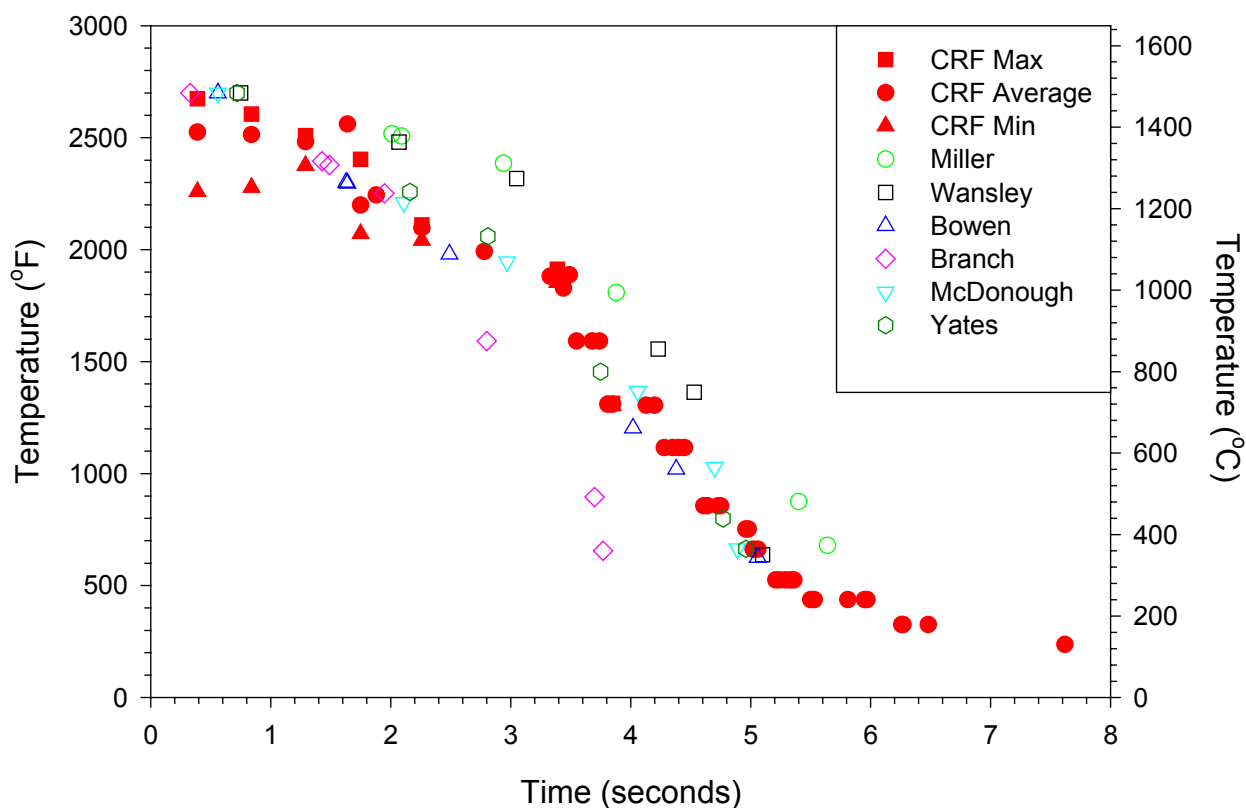


Figure A2. Combustion Research Facility (CRF) temperature/time Histories compared with those of full-scale Southern Company Services, coal-fired power plants.

Burner Assembly

The burner is mounted coaxially on the bottom of the furnace and is up-fired using natural gas, pulverized coal, any combination of the two or any other fuel that can be finely divided and transported to the pulverized coal silo. It is equipped with a flow control system for secondary air flow and a set of registers, which impart swirl to the secondary air, separate from the flow control. The secondary air and the primary air-coal mixture enter the furnace through a refractory quarl with a 25° half angle. Two clean-out ports are provided in this section, to allow

bottom ash to be periodically removed from the furnace. A closed-circuit television camera with a control-room monitor allows constant monitoring of the view of the flame from the top of the furnace. A low NO_x firing system, consisting of a generic dual-register burner and an overfire air system, can be installed to simulate several combinations of low NO_x firing.

Convective Sections

The combustion gases exit the vertical furnace through a horizontal convection pass, which is designed to remove a substantial part of the heat from the flue gases. The extraction of heat is designed in order to simulate the time-temperature profile found in a utility boiler. A series of three air-cooled tube banks are installed in the convective pass, and the air cooling is used to control either the temperature profile of the flue gases or the tube metal surface temperatures for fouling/ash deposition studies. A cross-flow tubular air preheater follows the convective tube banks and is used to preheat the primary and secondary air. Finally, four air-to-flue-gas recuperators are used to cool the flue gas down to a nominal 300°F before the flue gas enters the pollution control devices.

The convective section is 1.5 feet x 1.5 feet x 22 feet, providing gas velocities of 10 to 20 m/s (30 to 60 ft/s) and residence times of 0.4 to 0.8 seconds, again depending upon the firing rate. The design temperature range for the convective section is 1200 to 650°C (2200 to 1200°F).

Computer Data Acquisition and Control System

The facility is controlled and monitored by networked combined digital control system (DCS) and data acquisition computers, managed by Yokogawa CS-1000 system software that runs under the Windows NT operating system. This DCS performs all process control for the facility and allows complex feed-forward and calculated variable control. This computer control also performs the monitoring needed for safe operation of combustion equipment, including flame scanning and interlocks, automatic startup, and automatic shutdown of the entire facility. Process data acquisition and storage is accomplished within the Yokogawa software.

CEM System

A complete, extractive, continuous emissions monitoring (CEM) system is installed in the facility.

Pollution Control Equipment

Test equipment available for use at the Combustion Research Facility include an Electrically Stimulated Fabric Filter, a dry wall Electrostatic Precipitator, and a fluidized semi-dry / dry desulfurization system.

Mercury Measurements

An advanced and improved version of the PS Analytical mercury monitor is currently set up at the CRF, including a *spike and recovery* system. Accurate and precise mercury speciation measurements are key to a fundamental mercury speciation and capture investigation. As a result of extensive engineering, SRI can now measure mercury speciation within a maximum

uncertainty of 5%, which capability is essential to the success of this project. Furthermore, an advanced *spike and recovery* system makes it possible to validate the correctness of the mercury speciation numbers measured and correct for errors that occur.

Spike and Recovery System

The *spike and recovery system* is a first of its kind prototype, provided to SRI by PS Analytical, as a result of extensive discussions with various PSA personnel. The adaptation of this *spike and recovery* system to allow spiking at the tip of the APOGEE Scientific QGIS probe was performed entirely by SRI personnel. The spike of mercury is introduced into the tip of the APOGEE Scientific QGIS probe far enough downstream from the inlet to prevent losses to the duct and far enough upstream of the porous annulus to allow complete mixing before the sampled gas is pulled through the porous frit. A relatively small quantity of air is used to carry the mercury spike to the probe. Therefore, dilution is insignificant and the general flue-gas composition is undisturbed. The main impact of the spike is simply to increase the concentration of mercury in the sampled gas. The concentration of mercury in the spike stream is generated by controlling the flow rate, pressures and temperatures of air in and through a mercury reservoir chamber. This prototype system will be improved upon, based on the information learned from this and other experiments. In addition, SRI uses a parallel Hg-source for the *spike and recovery* system, involving permeation tubes, allowing a check on the source calibration. Without spike and recovery, all Hg-monitor data reported in the literature must be regarded as highly suspect, especially with regards to Hg-speciation.

Electrostatic Precipitator

A four-field dry-wall electrostatic precipitator has been recently installed in the facility. With an interior that is nominally 1.4-m (4½') high by 0.6-m (2') wide by 4.9-m (16') long, the precipitator provides a maximum plate area of approximately 13 m² (144 sq.ft) for an ESP sizing factor of 120 sq.ft /kacfm. Plate width can be changed, allowing plate spacings up to a maximum of 0.6-m (24").

Particles are charged by a rigid electrode array. The discharge electrodes are suspended from high voltage structures located in the area above the gas passage. The high voltage structures are suspended from insulators, electrically isolating them from the precipitator casing. The discharge electrodes are attached to the upper high-voltage frame and extend down through the gas passages. They are aligned by the lower high-voltage frame. This lower high-voltage frame is suspended from the rigid discharge electrodes. The discharge electrodes are centered in the gas passages, with anti-sway mechanisms attached to the lower high-voltage frame to keep it from moving in the gas stream.

As an aid to gas distribution, turning vanes, perforated plates, and baffles are used at the inlet and outlet of the precipitator chamber. The purpose is to provide uniform velocity distribution across the precipitator cross-section. Impulse gravity impact rappers are used to remove dust deposits from collecting surfaces. The rappers are located on the precipitator roof. The plunger is allowed to fall, striking the rapper bar connected to a bank of collecting surfaces within the precipitator. The resulting shock dislodges the accumulated dust. Precipitator rapping is controlled through a microprocessor-based programmable controller.

Fluidized Bed Desulfurization Reactor

Figure A3 contains a schematic of the Fluidized Bed Desulfurization Reactor (FBDR) system. The flue gas from the furnace enters the bottom of the reactor and passes upward through a venturi section. At the top of the venturi section, sorbent is introduced. Two feet above this and approximately 0.1 seconds of residence time after sorbent injection, water is injected into the duct, which significantly cools the gas. The sulfur dioxide in the flue gas reacts with the sorbent. The flue gas and solids pass from the FBDR to the baghouse, where virtually 100 % of the solids are captured. The cleaned gas exits the baghouse to the fan and stack. The reactor was designed to provide approximately 1½ -2 seconds reaction time before collection on the fabric filters. A second port is available at the top of the reactor, which can be used to reduce the reaction time available to approximately ¾-1 seconds. The FBDR is equipped with a sorbent recycling loop and may be operated in once-through or continuous recycling mode.

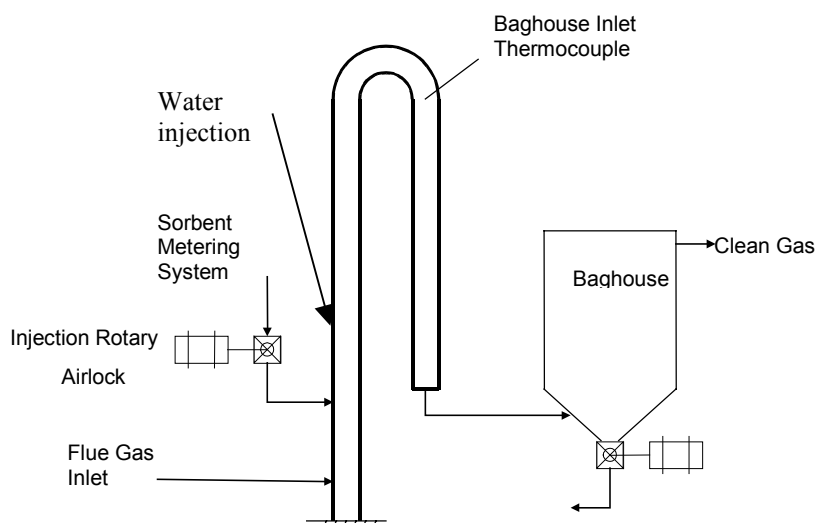


Figure A3. Schematic Flow Diagram of the Fluidized Bed Desulfurization Reactor (FBDR).

Permit Equipment

Particulate emissions are controlled by an Aeropulse pulse-jet baghouse, while sulfur dioxide emissions are controlled by an Indusco packed-column caustic scrubber. The pulse-jet baghouse and scrubber are required for the air quality permit of the facility issued by the Jefferson County Board of Health and are always on-line.

Combustor Operations

A routine facility operation is usually completed in one week, beginning at 8:00 am on Monday morning and ending at 5:00 PM on Friday afternoon. To facilitate start of testing on Monday morning the furnace is usually started on Sunday evening, firing with natural gas to heat up the system before switching to coal. It usually requires 12 hours before thermal equilibrium is achieved.

APPENDIX B

NON-CORRELATING GRAPHS

Figure B1 illustrates the NON-relationship between gas-phase mercury speciation and flue-gas moisture content. The other graphs in this appendix illustrate NON-correlations of different parameters with mercury oxidation and capture.

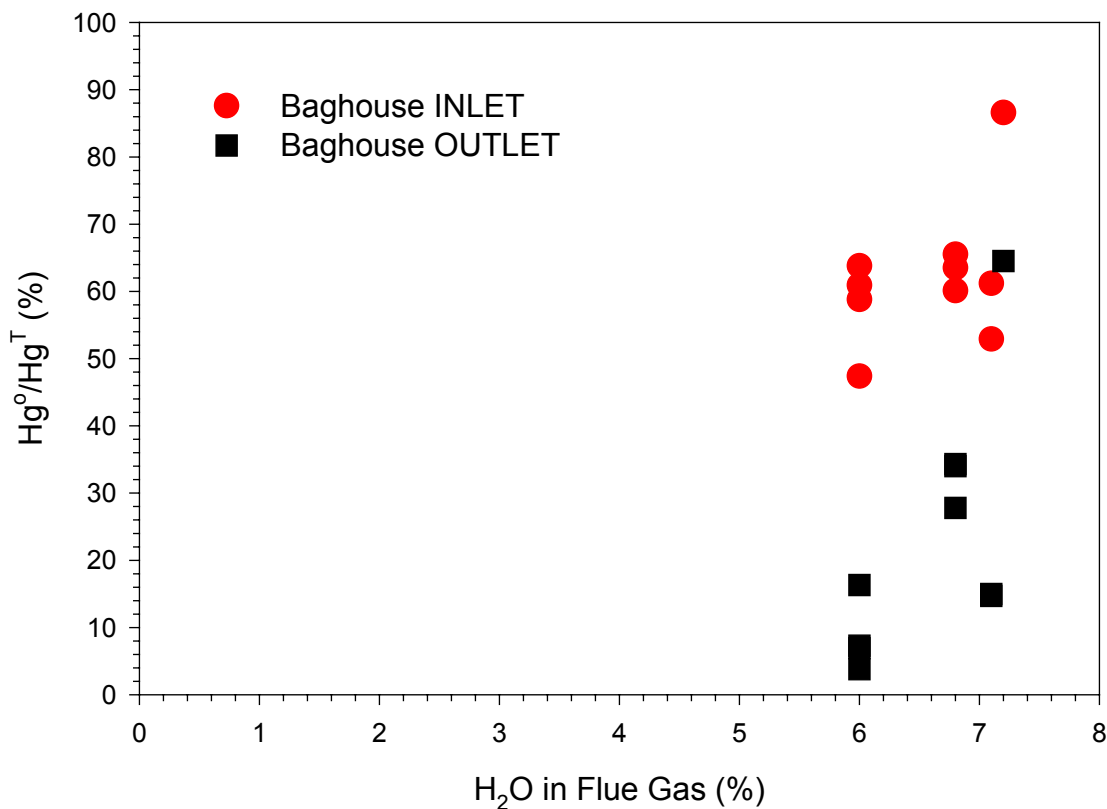


Figure B1. Fraction of elemental mercury versus flue-gas moisture content.

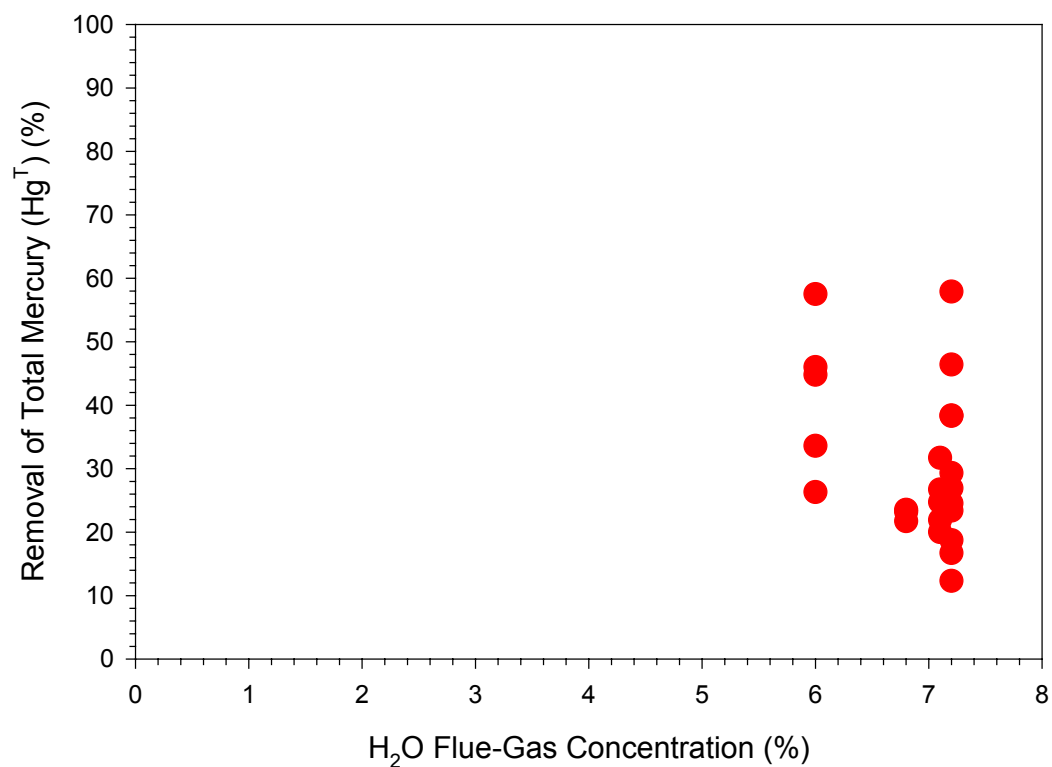


Figure B2. Mercury Capture versus moisture in the flue gas.

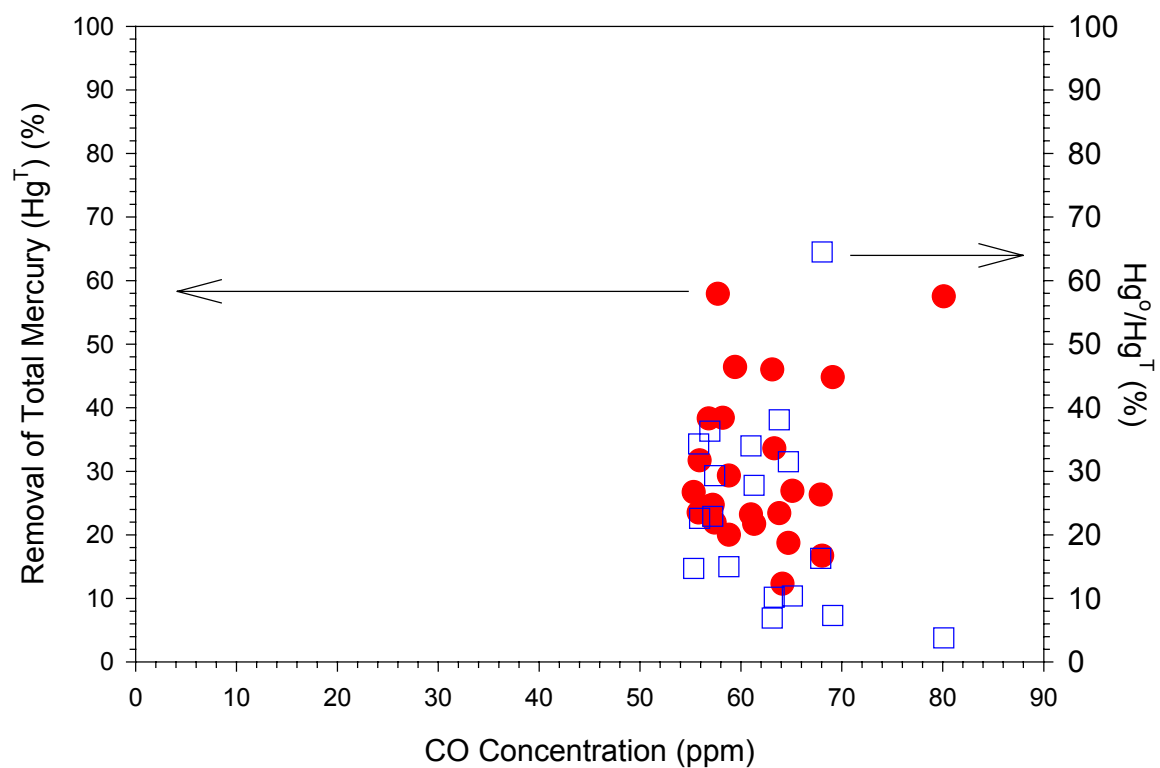


Figure B3. Mercury oxidation and capture at baghouse outlet versus flue gas CO.

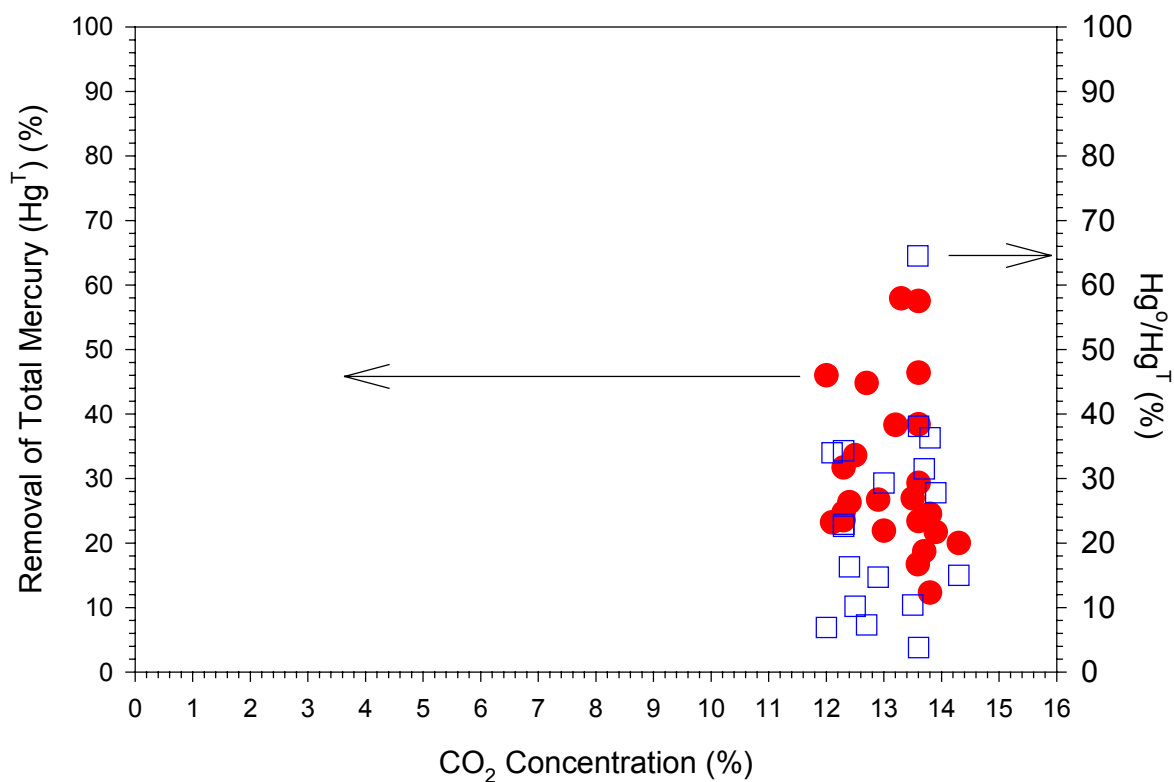


Figure B4. Mercury oxidation and capture at baghouse outlet versus flue gas CO₂.

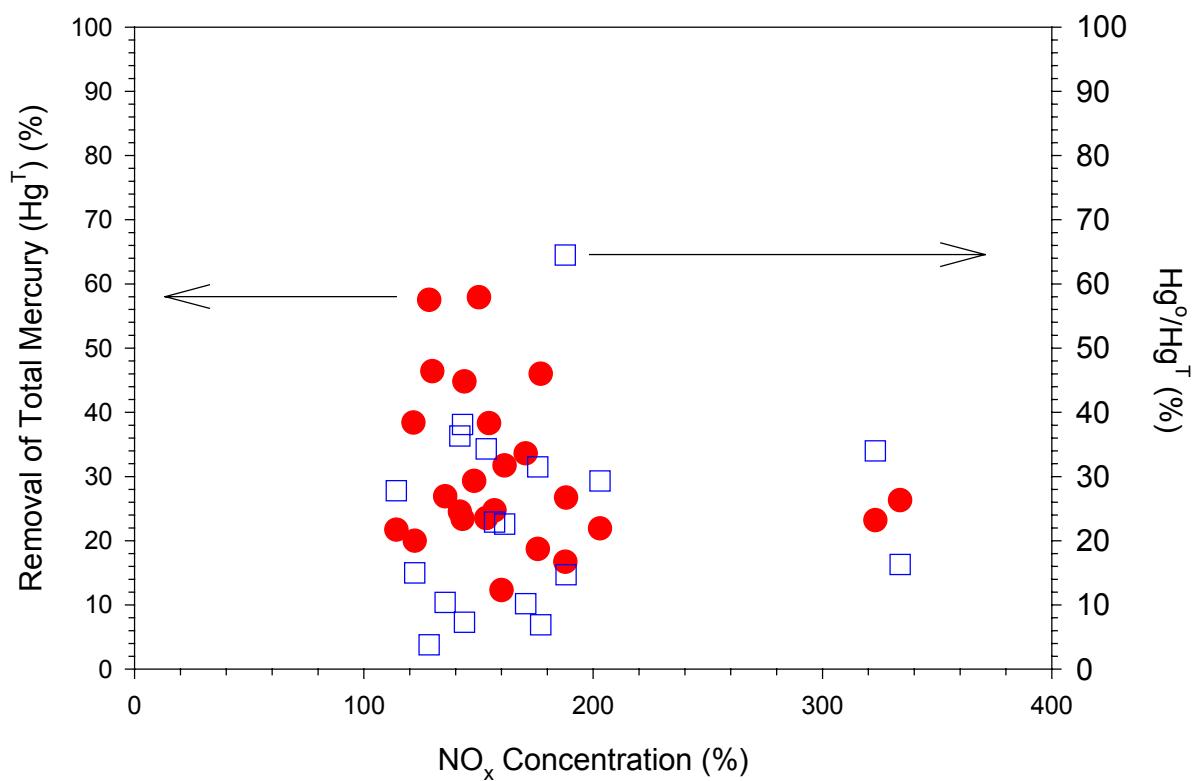


Figure B5. Mercury oxidation and capture at baghouse outlet versus flue gas NO_x.

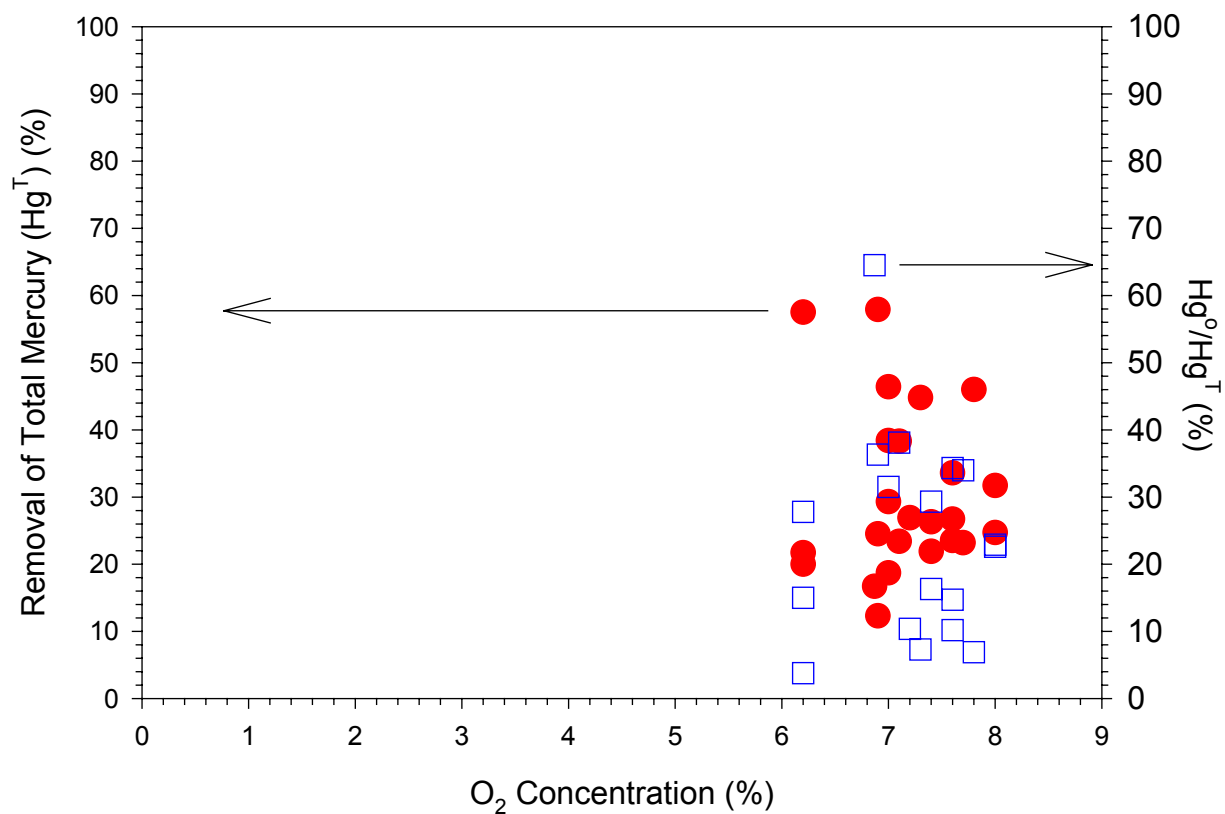


Figure B6. Mercury oxidation and capture at baghouse outlet versus flue gas O₂.

APPENDIX C

RUN CONDITIONS AND DATA

The objective in the presenting the data in this appendix is to provide enough information to allow fundamental modelers access to all of the information they need to compare their theoretical predictions to experimental data. The data here presented should be sufficient to allow comparison with detailed fundamental models of mercury speciation for coal-fired applications, without recourse to any assumptions or need to obtain additional information elsewhere.

Table C1. Run conditions

Run Cond. #	Coal Type			Choctaw Ash / Hydrated lime Injection Condition
	Powder River Basin	Blacksville	Choctaw America	
1	100%	---	---	---
2	100%	---	---	---
3	100%	---	---	---
4	100%	---	---	---
5	100%	---	---	---
6	100%	---	---	---
7	100%	---	---	---
8	100%	---	---	---
9	100%	---	---	15 lbs/hr Choctaw America Ash into Baghouse
10	100%	---	---	15lb/hr 50% CA ash/50% HL in baghouse
11	100%	---	---	15lb/hr 20% CA ash/80% HL in baghouse
12	80%	20%	---	---
13	80%	20%	---	---
14	80%	20%	---	---
15	80%	20%	---	---
16	90%	10%	---	---
17	90%	10%	---	---
18	90%	10%	---	10 lb/hr hydrated lime into baghouse
19	90%	10%	---	15 lb/hr hydrated lime into convection pass
20	90%	10%	---	15 lb/hr hydrated lime into convection pass
21	90%	---	10%	---
22	90%	---	10%	---
23	90%	---	10%	---
24	^a 60%	^a 40%	---	---

CA = Choctaw America, HL = Hydrated Lime

a. This blend was fired for only a few hours at the end of the test week. The actual ash composition was similar to the 20% BV/80% PRB blend, due to residual ash and mixing from the previous test conditions.

Table C2. Run conditions continued.

Run Con d. #	HCl in Flue Gas (ppmv)	Baghouse Temperature (°F)	FEO (%)	Overfire Air (%)	Coal Feed Rate Lbs/hr
1	1.1 +/- 0.1	280-260	3.5	15	365 +/- 3
2	33 +/- 2	280-260	3.5	15	364 +/- 3
3	105 +/- 3	280-260	3.5	15	364 +/- 3
4	185 +/- 1	280-260	3.5	15	364 +/- 3
5	1.1 +/- 0.1	280-260	3.5	15	364 +/- 3
6	1.1 +/- 0.1	337-300	3.5	15	363 +/- 3
7	1.1 +/- 0.1	337-300	3.5	15	364 +/- 3
8	1.1 +/- 0.1	337-300	3.5	15	364 +/- 3
9	1.1 +/- 0.1	337-300	3.5	15	364 +/- 3
10	1.1 +/- 0.1	337-300	3.5	15	364 +/- 3
11	1.1 +/- 0.1	337-300	3.5	15	364 +/- 3
12	13 +/- 0.8	280-260	4.5	15	333 +/- 2
13	13 +/- 0.8	337-300	4.5	15	333 +/- 2
14	13 +/- 0.8	280-260	3.5	15	333 +/- 2
15	13 +/- 0.8	280-260	2.5	15	335 +/- 2
16	8 +/- 1	280-260	2.5	15	359 +/- 2
17	8 +/- 1	280-260	4.5	15	359 +/- 2
18	8 +/- 1	280-260	4.5	15	359 +/- 2
19	8 +/- 1	280-260	4.5	15	359 +/- 3
20	8 +/- 1	337-300	4.5	15	360 +/- 2
21	2.6 +/- 0.1	280-260	4.5	15	360 +/- 2
22	2.6 +/- 0.1	280-260	2.5	15	360 +/- 2
23	2.6 +/- 0.1	280-260	4.5	0.0	361 +/- 2
24	15 +/- 2.6	280-260	4.5	0.0	330 +/- 2

Table C3. Mercury speciation measurements.

Run Cond. #	Hg ^T Mass Balance $\mu\text{g}/\text{m}^3$	Hg ^o Baghouse Inlet $\mu\text{g}/\text{m}^3$	Hg ^T Baghouse Inlet $\mu\text{g}/\text{m}^3$	Hg ^o Baghouse Outlet $\mu\text{g}/\text{m}^3$	Hg ^T Baghouse Outlet $\mu\text{g}/\text{m}^3$
1	7.5 +/- 0.6	5.84 +/- 0.58	6.74 +/- 0.61	4.35 +/- 0.14	6.25 +/- 0.27
2	7.5 +/- 0.6	5.20 +/- 0.15	7.18 +/- 0.36	2.26 +/- 0.17	6.10 +/- 0.54
3	7.5 +/- 0.6	---	7.23 +/- 0.45	---	5.48 +/- 0.52
4	7.5 +/- 0.6	---	---	---	6.42 +/- 0.64
5	7.5 +/- 0.6	---	---	---	6.58 +/- 0.07
6	7.5 +/- 0.6	6.05 +/- 0.08	7.58 +/- 0.23	2.75 +/- 0.14	5.66 +/- 0.58
7	7.5 +/- 0.6	---	---	---	4.68 +/- 0.35
8	7.5 +/- 0.6	“	“	2.40 +/- 0.09	5.36 +/- 0.28
9	7.5 +/- 0.6	“	“	1.14 +/- 0.11	3.19 +/- 0.70
10	7.5 +/- 0.6	“	“	1.36 +/- 0.17	4.06 +/- 0.06
11	7.5 +/- 0.6	“	“	2.11 +/- 0.08	4.67 +/- 0.10
12	7.3 +/- 0.5	3.49 +/- 0.17	5.94 +/- 0.08	0.41 +/- 0.08	3.94 +/- 0.20
13	7.3 +/- 0.5	3.63 +/- 0.38	6.47 +/- 0.37	0.66 +/- 0.07	4.85 +/- 0.14
14	7.3 +/- 0.5	4.55 +/- 0.16	7.13 +/- 0.26	0.52 +/- 0.08	4.03 +/- 0.17
15	7.3 +/- 0.5	3.67 +/- 0.03	6.03 +/- 0.13	0.23 +/- 0.04	3.10 +/- 0.40
16	8.1 +/- 0.9	4.10 +/- 0.27	7.75 +/- 0.25	1.16 +/- 0.18	6.48 +/- 0.32
17	8.1 +/- 0.9	4.53 +/- 0.35	7.40 +/- 0.41	1.09 +/- 0.25	5.94 +/- 0.27
18	8.1 +/- 0.9	4.43 +/- 0.14	7.61 +/- 0.21	2.23 +/- 0.31	6.33 +/- 0.29
19	8.1 +/- 0.9	4.30 +/- 0.18	6.50 +/- 0.14	1.47 +/- 0.12	5.53 +/- 0.16
20	8.1 +/- 0.9	4.15 +/- 0.08	7.19 +/- 0.07	1.65 +/- 0.10	6.10 +/- 0.07
21	8.1 +/- 0.9	4.60 +/- 0.26	7.24 +/- 0.41	2.48 +/- 0.18	6.20 +/- 0.52
22	8.1 +/- 0.9	4.27 +/- 0.23	7.11 +/- 0.34	1.98 +/- 0.38	6.34 +/- 0.46
23	8.1 +/- 0.9	4.45 +/- 0.31	6.79 +/- 0.43	2.31 +/- 0.09	6.22 +/- 0.27
24	7.1 +/- 0.7	2.61 +/- 0.07	5.51 +/- 0.48	0.90 +/- 0.23	5.23 +/- 0.12

Table C4. Major flue gas species.

Run Cond. #	NO _x (ppm)	SO ₂ (ppm)	CO (ppm)	CO ₂ (%)	O ₂ (%)	H ₂ O (%)
1	187.9+/-12.4	172.7+/-10.1	68.1+/-4.5	13.6+/-0.2	6.9+/-0.14	7.2
2	175.9+/-20	178+/-20.7	64.7+/-5.3	13.7+/-1.0	7.0+/-0.13	7.2
3	135.5+/-9.9	189.3+/-20	65.1+/-4.3	13.5+/-0.4	7.2+/-0.20	7.2
4	143.1+/-23.9	156.8+/-24.6	63.8+/-3.4	13.6+/-0.3	7.1+/-0.20	7.2
5	160+/-8.7	70.8+/-42.2	64.1+/-3.3	13.8+/-0.3	6.9+/-0.10	7.2
6	141.9+/-9.7	175.1+/-4.9	56.9+/-3.1	13.8+/-0.3	6.9+/-0.20	7.2
7	154.6+/-60.3	182+/-54.1	56.8+/-11	13.2+/-1.7	7.1+/-0.20	7.2
8	148.1+/-8.5	202.4+/-17.1	58.8+/-2.8	13.6+/-0.3	7.0+/-0.10	7.2
9	150.2+/-72	193.6+/-59.9	57.7+/-13.7	13.3+/-1.8	6.9+/-0.10	7.2
10	129.9+/-8.5	185.2+/-10.9	59.4+/-2.9	13.6+/-0.2	7.0+/-0.10	7.2
11	121.6+/-4.2	197+/-5.3	58.2+/-3.3	13.6+/-0.2	7.0+/-0.20	7.2
12	177.2+/-10.9	603.3+/-21.8	63.1+/-3.2	12.0+/-0.3	7.8+/-0.20	6
13	170.6+/-10.5	615.4+/-10	63.3+/-3.9	12.5+/-0.3	7.6+/-0.20	6
14	143.9+/-6.7	661+/-13.2	69.1+/-3.7	12.7+/-0.2	7.3+/-0.20	6
15	128.5+/-4.8	702+/-14.6	80.1+/-5.6	13.0+/-0.3	6.2+/-0.10	6
16	122.2+/-6.6	494.2+/-12.5	58.8+/-3.1	14.3+/-0.2	6.2+/-0.10	7.1
17	188.2+/-8.9	510.5+/-10.7	55.3+/-2.9	12.9+/-0.2	7.6+/-0.10	7.1
18	203+/-22.6	536.6+/-9.9	57.4+/-3.2	13.0+/-0.2	7.4+/-0.20	7.1
19	161.4+/-13.4	479.7+/-7.8	55.9+/-3.3	12.3+/-0.1	8.0+/-0.10	7.1
20	157+/-8.8	451.6+/-9.1	57.2+/-3.4	12.3+/-0.1	8.0+/-0.10	7.1
21	153.4+/-11.6	365.7+/-28	55.8+/-3.1	12.3+/-0.2	7.6+/-0.10	6.8
22	114.2+/-5	401.9+/-4.3	61.3+/-3.0	13.9+/-0.2	6.2+/-0.10	6.8
23	323.1+/-10.2	332.1+/-23.5	61+/-3.6	12.1+/-0.1	7.7+/-0.10	6.8
24	333.9+/-17.1	688.8+/-14.6	67.9+/-2.9	12.4+/-0.2	7.4+/-0.10	6

Table C5. Mineral analysis, unburned carbon (UBC), and loss on ignition (LOI) of isokinetically sampled ash samples.

Component	Conditions 1-8	Cond. 12-13	Condition 14	Condition 15	Condition 16
% Li ₂ O	0.01	0.02	0.02	0.02	0.04
% Na ₂ O	2.4	1.7	1.7	1.7	1.8
% K ₂ O	0.61	0.62	0.70	0.73	0.70
% MgO	5.3	4.2	3.8	3.7	6.2
% CaO	27.3	22.2	21.6	21.3	21.7
% Fe ₂ O ₃	7.1	8.8	9.3	9.4	8.4
% Al ₂ O ₃	18.2	20.3	20.6	20.9	20.0
% SiO ₂	29.6	33.7	34.5	34.5	32.5
% TiO ₂	1.7	1.7	1.6	1.6	2.0
% P ₂ O ₅	1.3	1.0	1.1	1.2	2.3
% SO ₃	3.7	4.2	4.3	3.8	5.0
% LOI	0.23	0.90	0.94	1.6	0.56
% UBC	0.07 – 0.11	0.71 – 0.73	0.95 +/- 0.04	1.45 +/- 0.03	0.33 +/- 0.02

Table C6. Mineral analysis, unburned carbon (UBC), and loss on ignition (LOI) of isokinetically sampled ash samples -- continued.

Component	Condition 17	Condition 21	Condition 22	Condition 23	Condition 24
% Li ₂ O	0.02	0.02	0.02	0.02	0.02
% Na ₂ O	1.9	2.0	2.1	2.1	1.7
% K ₂ O	0.58	0.58	0.62	0.59	0.74
% MgO	4.2	4.3	4.5	4.4	4.0
% CaO	22.8	25.2	25.0	25.2	22.2
% Fe ₂ O ₃	7.9	8.0	7.9	7.8	8.7
% Al ₂ O ₃	21.2	20.1	20.8	20.7	21.3
% SiO ₂	31.2	31.0	30.1	29.9	34.1
% TiO ₂	1.6	1.5	1.7	1.8	1.6
% P ₂ O ₅	1.5	1.4	1.6	1.5	0.95
% SO ₃	5.1	4.6	4.0	4.8	3.4
% LOI	0.36	0.69	0.60	0.59	0.92
% UBC	0.47 +/- 0.01	0.34 +/- 0.02	0.57 +/- 0.01	0.27 +/- 0.01	0.52 +/- 0.01

Table C7. Coal heating values, mercury, and chlorine contents.

Run Cond. #	Coal Blend Moisture (%)	Heating Value (dry) (BTU/Lb)	Mercury in Coal ($\mu\text{g/g}$)	Mercury in Ash Samples ($\mu\text{g/g}$)	Chlorine in Coal ($\mu\text{g/g}$)	Chlorine in Ash Samples ($\mu\text{g/g}$)
1	12.3	11,107	0.081	---	< 0.010	---
2	12.7	11,074	0.089	---	< 0.010	---
3	---	---	---	0.116	< 0.010	1108
4	14.0	11,149	0.095	0.227	< 0.010	4345
7	---	---	---	0.114	< 0.010	3053
8	13.4	11,075	0.097	---	< 0.010	---
12	11.1	11,957	0.097	0.522–0.564	148	273
13	13.0	12,110	0.092	0.429	206	---
14	12.4 – 14.3	12,167	0.086	0.081	226	---
15	13.7	12,160	0.092	1.036	193	---
16	15.8	11,753	0.095	0.408	140	---
17	12.8	11,679	0.095	0.581	140	---
18	12.8	11,679	0.089	---	141	---
19	15.7	11,765	0.102	---	131	---
20	15.7	11,765	0.095	---	144	---
21	14.8	11,850	0.106	0.114	85	---
22	14.8	11,850	0.106	0.632	85	---
23	14.8	11,850	0.106	0.223	85	176
24	7.1 – 8.8	12,224	0.087-0.099	0.364	246-279	---

Table C8. Coal blend fractions.

Run Cond. #	Coal Blends Based on Mass Fraction			Coal Blends Based on Heating Value		
	X PRB (%)	X BV (%)	X CA (%)	X PRB (%)	X BV (%)	X CA (%)
1	100	---	---	100	---	---
2	100	---	---	100	---	---
3	100	---	---	100	---	---
4	100	---	---	100	---	---
7	100	---	---	100	---	---
8	100	---	---	100	---	---
12	73.1	26.9	---	66.3	33.7	---
13	75.7	24.3	---	69.3	30.7	---
14	72.5 – 78.5	21.5 – 27.5	---	65.6 – 72.6	27.4 – 34.4	---
15	76.8	23.2	---	70.6	29.4	---
16	93.2	6.8	---	90.8	9.2	---
17	85.3	14.7	---	80.8	19.2	---
18	85.3	14.7	---	80.8	19.2	---
19	92.6	7.4	---	90.0	10.0	---
20	92.6	7.4	---	90.0	10.0	---
21	89.7	---	10.3	85.7	---	14.3
22	89.7	---	10.3	85.7	---	14.3
23	89.7	---	10.3	85.7	---	14.3
24	53.2 – 60.6	39.4 – 46.8	---	45.2 – 52.8	47.2 – 54.8	---

Table C9. Temperature/time history information for low baghouse temperature condition.

Distance (ft)	Res. Time (s)	Temperature (°C)	CRF Location
0	---	500	Quarl Tip
0.42	0.00	881	
1.42	0.21	901	
2.46	0.36	1279	
6.54	0.81	1312	
10.63	1.24	1244	
13.71	1.59	1405	
14.71	1.70	1204	Overfire Air Ports
15.71	1.81	1229	
18.79	2.17	1152	
22.88	2.65	1018	
26.96	3.19	889	Furnace Exit (FEO applies here)
28.58	3.24	884	
30.08	3.29	906	
31.08	3.35	884	
33.50	3.41	804	
37.08	3.54	804	
38.08	3.60	804	
40.50	3.66	675	
41.42	3.70	675	
47.92	3.97	675	
48.92	4.04	675	
51.33	4.11	613	
52.83	4.18	613	
53.83	4.22	613	
54.83	4.27	613	
55.83	4.42	496	
56.33	4.44	496	
57.83	4.52	496	
58.17	4.54	496	
62.83	4.73	400	
63.17	4.76	400	
63.67	4.79	363	
64.17	4.83	363	
66.83	4.97	286	
67.17	4.99	286	
67.67	5.03	286	
68.17	5.07	286	Start of Last Set of Heat Exchangers
68.50	5.10	286	
70.83	5.23	235	
71.17	5.25	235	
75.00	5.51	231	(Due to slow air in-leakage from the convection pass to the baghouse, the flue gas oxygen at the baghouse is at the values measured by the CEMs (see Table C4))
77.00	5.63	231	
77.33	5.66	231	
82.00	5.92	163	
82.33	5.93	163	
88.50	6.11	163	
121.83	7.08	142	Baghouse Inlet
135.17	7.50	127	Baghouse Outlet

Table C10. Temperature/time history information for high baghouse temperature condition.

Distance (ft)	Res. Time (s)	Temperature (°C)	CRF Location
0	---	500	Quarl Tip
0.42	0.00	881	
1.42	0.21	901	
2.46	0.36	1279	
6.54	0.81	1312	
10.63	1.24	1244	
13.71	1.59	1405	
14.71	1.70	1204	Overfire Air Ports
15.71	1.81	1229	
18.79	2.17	1152	
22.88	2.65	1018	
26.96	3.19	889	Furnace Exit (FEO applies here)
28.58	3.24	884	
30.08	3.29	906	
31.08	3.35	884	
33.50	3.41	804	
37.08	3.54	804	
38.08	3.60	804	
40.50	3.66	675	
41.42	3.70	675	
47.92	3.97	675	
48.92	4.04	675	
51.33	4.11	613	
52.83	4.18	613	
53.83	4.22	613	
54.83	4.27	613	
55.83	4.42	496	
56.33	4.44	496	
57.83	4.52	496	
58.17	4.54	496	
62.83	4.73	400	
63.17	4.76	400	
63.67	4.79	363	
64.17	4.83	363	
66.83	4.97	286	
67.17	4.99	286	
67.67	5.03	286	
68.17	5.07	286	
68.50	5.10	286	Start of Last Set of Heat Exchangers
70.83	5.23	285	
71.17	5.25	275	
75.00	5.51	275	(Due to slow air in-leakage from the convection pass to the baghouse, the flue gas oxygen at the baghouse is at the values measured by the CEMs (see Table C4))
77.00	5.63	275	
77.33	5.66	275	
82.00	5.92	193	
82.33	5.93	193	
88.50	6.11	193	
121.83	7.08	170	Baghouse Inlet
135.17	7.50	150	Baghouse Outlet